6-17-2010

Characterization and Evaluation of Performance of a Whole-Body Human Exposure Chamber

Luis F. Pieretti
University of South Florida

Characterization and Evaluation of Performance of a Whole-Body Human Exposure Chamber

by

Luis F. Pieretti

A dissertation submitted in partial fulfillment
of the requirements for the degree of
Doctor of Philosophy
Department of Environmental and Occupational Health
College of Public Health
University of South Florida

Major Professor: Yehia Y. Hammad, Sc.D.
Thomas E. Bernard, Ph.D.
Steven P. Mlynarek, Ph.D.
Yangxin Huang, Ph.D.

Date of Approval:
June 17, 2010

Keywords: Inhalation Challenge, Generation of Aerosols, Exposure System, Aerosols, Particulates

Dedication

This work is dedicated to my wife, Nelmarie, whose love, support and encouragement made possible the completion of this dissertation, and to my parents, Luis Alfredo and Sylvia, for always believing in me.

Acknowledgments

I thank Dr. Yehia Hammad for his patience, wisdom and guidance during my doctoral years. His enthusiasm for and knowledge of the industrial hygiene field made my journey an easier one to travel. I also thank Dr. Steve Mlynarek for his encouragement, support and valuable advice.

I thank Dr. Thomas Bernard and Dr. Yangxin Huang for their support and suggestions regarding this research.

I also acknowledge Mr. Robert Nesbit and Mrs. Charlene Vespi for their support and loan of equipment.

I'm extremely grateful to the National Institute for Occupational Safety and Health for supporting this project under training grant T42-OH008438.

Table of Contents

List of Tables

List of Figures

List of Equations

List of Acronym, Abbreviations and Symbols

A	In physical dimension, area
α	Greek letter alpha, the confidence level for a statistical test
cm	Centimeter
CFM	Cubic feet per minute
ft^3/min	Cubic feet per minute
CO_2	Carbon dioxide
CV	Coefficient of variation
d_a	Aerodynamic diameter of a particle
η	Greek letter ETA, absolute viscosity
ft^2	Area expressed as square feet
G	The rate of generation
g	Acceleration due to gravity
gm	Gram
HEPA	High-efficiency particulate air (filter)
in^2	Area expressed as square inch
K	Mixing factor
K_m	Ratio of mixing rate constant
L	Liter
ln	Natural logarithm
L/min	Flowrate expressed as liters per minute
m^3	Volume expressed as cubic meter

µg	Microgram
µm	Micrometer
mg	Milligram
min	Minute
p	Probability
PVC	Polyvinyl chloride
Q	Volumetric flowrate
QCM	Quartz crystal microbalance
R^2	The coefficient of determination
ρ	Greek letter Rho, density
SD	Standard deviation
TEOM	Tapered Element Oscillating Microbalance
V_{ts}	Terminal settling velocity of a particle
VP	Velocity pressure
w.g.	Pressure expressed as inches of water gauge

Characterization and Evaluation of Performance of a Whole-Body Human Exposure Chamber

Luis F. Pieretti

ABSTRACT

The purpose of this study was to characterize and evaluate the performance of a whole-body human exposure chamber for controlled test atmospheres of gases and particulates. The chamber was constructed from Plexiglass, has a volume of 75 ft^3, operated at a flowrate of 33.8 CFM, and both the makeup and exhaust air are HEPA filtered. Fly ash dust was generated using a Wright Dust Feeder. An elutriator was used to eliminate particles larger 8 µm aerodynamic diameter from the airstream. A direct reading instrument, the Rupprecht and Patashnick PM-10 TEOM, was used for determination of particle concentration. Particle size distributions were determined by a QCM cascade impactor. Data from gravimetric analysis were used to test for the evenness of dust concentrations in the chamber. CO_2 is used as a representative gas and its concentration was measured using the Metrosonics aq-5000.

Total dust concentrations as measured by the TEOM, in $\mu g/m^3$, at 0.2, 0.4, 0.6 and 1.6 RPMs of the Wright Dust Feeder, were 110 $\pm$ 2.8, 173 $\pm$ 8.5, 398 $\pm$ 20 and 550 $\pm$ 17, respectively. For these RPMs, particle size distributions were associated with a MMD of 1.27 µm and a GSD of 2.35, a MMD of 1.39 and a GSD of 2.22, a MMD of 1.46 and a GSD of 2.08, a MMD of 1.15 and a GSD of 2.2, respectively. Total dust concentrations as measured by gravimetric analysis, in $\mu g/m^3$, at 0.2, 0.4, 0.6 and 1.6 RPMs of the Wright Dust Feeder, were 135 $\pm$ 21, 200 $\pm$ 35, 333 $\pm$ 18 and 891 $\pm$ 27, respectively. Similar results were found for the inhalable fraction and lower concentrations were found

for the respirable fraction. Dust concentrations measured at different points within the chamber showed uniform distribution with a variability less than 10%. Similarly, the particle size distributions were found to be consistent across the different RPMs settings. Regarding carbon dioxide, its concentration was straightforward and the measured and theoretical maximum concentration levels were in agreement.

The performance of this whole-body human exposure chamber has been characterized and evaluated for low levels of particles and gases and now it is a valuable research tool for inhalation challenge studies.

Chapter One

Introduction

Purpose of this study

The purpose of this study is to characterize and evaluate the performance of a whole-body human exposure chamber located in the Breath Laboratory of the Sunshine Education and Research Center at the College of Public Health, University of South Florida. This inhalation challenge system was designed by Yehia Y. Hammad, Sc.D. The characterization and evaluation will provide the answers to the following questions.

1. What is the concentration of the test atmosphere at different rates of generation in the inhalation challenge system?
2. What is the particle size distribution of the test material at different rates of generation?
3. Are there any differences among the particle size distributions of the test material obtained at different rates of generation?
4. Are there any differences among the concentration levels of the test atmosphere across the exposure chamber?

As a result of this study, researchers at the College of Public Health, University of South Florida will be able to use this exposure chamber as a tool in future inhalation challenge studies.

Types of Exposure Chambers

Inhalation challenge systems or exposure chambers can be broadly divided in two main categories: static exposure systems and dynamic exposure systems. Static exposure systems can be defined as systems where a certain amount of toxicant is injected in a closed environment. For these types of systems, the material can be inserted one time during the study or it can be re-circulated, depending on the purpose of the research. Contrary to static systems, dynamic systems can be defined as inhalation systems where the toxicant is constantly generated and delivered, and removed from the exposure chamber (McClellan & Henderson, 1995).

Dynamic exposure systems can be sub-divided in three main categories: nose-only, head-only and whole-body exposure chambers (Wong, 2007). Nose-only exposure systems are configured in a way that the toxicant is delivered directly to the nose of the animal or subject. This delivery method avoids deposition or dermal absorption of the test material and also minimizes the loss of the test material. Head-only exposure systems also avoid these problems. In this type of inhalation system, the head of the animal or subject is the only section of the body that is immersed in the test atmosphere. Head-only inhalation challenge systems are used when studies consider the ingestion of the test material (Willeke, 1980). Nose and head-only exposure systems are better suited when the test material is in short supply because of the delivery characteristics explained above (McClellan & Henderson, 1995). The main concerns when these types of inhalation systems are used with animals are the body heat buildup and stress created since the animals are restrained in a certain position (Wong, 2007), (McClellan & Henderson, 1995).

Contrary to nose and head-only exposure systems, whole-body exposure chambers require the complete body of the animal or subject to be immersed in the test atmosphere. This allows a natural delivery of the test material since the animal or subject just inhales and exhales in the controlled atmosphere without any attachments to their nose or head (Willeke, 1980), (Leong, 1981), (Wong, 2007). Since the whole body of the subject or animal is in the test atmosphere, the chances for dermal absorption and ingestion of the test material increase, making it difficult to differentiate among the effects of the inhaled, ingested and absorbed test material (Willeke, 1980). Another disadvantage of this type of exposure system is the loss of material. Not all the toxicant generated will be inhaled, thus this type of chamber requires more of the test material when compared to nose-only and head-only inhalation systems. Also, when using whole-body exposure chambers, some animals will tend to use their fur to protect their nose or the animals may band together and thus limit the exposure, making the nose-only or head-only exposure chambers more appropriate (Willeke, 1980), (Leong, 1981), (Wong, 2007).

Each of the three types of dynamic exposure systems has advantages and disadvantages. The suitability of each type of exposure system will depend on the requirements of the inhalation challenge study.

Buildup and Decay of Concentration

It is important to know the concentration of the toxicant at any given time while conducting an inhalation challenge study. If the rate of generation, air flowrate and volume of the system are known, it is possible to predict the concentration (C) at

equilibrium with Equation 1.

$$C = G/Q \quad (1)$$

Where “G” is the rate of generation of the toxicant, usually expressed in units of weight or volume per minute. “Q” is the average flowrate of the system and is expressed in units of volume per minute. If the rate of generation and flowrate are constant and the volume of the system is known, the concentration at any given time during the inhalation challenge study can be predicted with Equation 2.

$$C = KG/Q\ (1- e^{-QT/KV}) \quad (2)$$

The terms “G” and “Q” are the same as above. “T” is the time since the moment when the generation of the toxicant is started and is usually expressed in minutes. “V” is the volume of the exposure chamber. The term “K” is the unitless mixing factor. This mixing factor explains the effect of the mixing characteristics of the chamber and the test material. If there is complete, instantaneous mixing during an inhalation challenge study, the value of “K” becomes 1. When complete mixing is not achieved, the value of “K” is higher than 1 and may go as high as 10 (ACGIH, 2010). The mixing factor is associated with the flowrate and accounts for the amount of material that actually mixes with the air flow. This interaction affects the concentration at equilibrium and the time to reach such concentration.

The main factors that determine the time of the toxicant to reach equilibrium

concentration in an exposure chamber are the flowrate of the system, the volume of the exposure chamber and the mixing capabilities of the system. When these variables are constant, the equilibrium concentration is reached at the same time, regardless of the rate of generation.

When the generation of the test material is stopped and the flowrate of clean air is maintained constant, a dilution or purging process begins in the system. During this process, the concentration can be predicted theoretically with Equation 3.

$$C = C_0 (e^{-QT/KV}) \quad (3)$$

Where "C_0" is the concentration of the test material when generation is stopped. "Q", "K" and "V" are the same as discussed previously. In this case, the term "T" is the time from the moment the dilution or purging process starts. The degree mixing of the test material in the system will have the same effect as discussed before.

Generation of Test Material

Test material can be in the form of solid or liquid aerosols, and gases or vapors, depending on the requirements of the inhalation challenge study. For the dispersion of solid particles, the Wright Dust Feeder is the most used aerosol generator (Willeke, 1980) (Hinds, 1999). For this type of generator, the dust is compacted inside a cylinder, and this cylinder rotates on a scraper that is in a stationary position. As the cylinder rotates, the scraper removes a thin layer of the dust plug and clean air moves the scraped dust out of the generator at high velocity through a jet (Wright, 1950). This type of generator

works better with test material containing 90% or more of its particles in the respirable range (Wright, 1950), (Hinds, 1999), (Wong, 2007).

Another generator used for the dispersion of dust is the fluidized-bed dust generator. With this type of dust generator, the test material is constantly moved from a chamber with a chain conveyor into a bed fluidized by the passage of air. This fluidized bed contains bronze, stainless steel or nickel beads that will break the agglomerated dust by scrubbing action. The output of the dust generated will depend on the speed of the chain conveyor, which is controlled by the user. The small aerosols are separated by an elutriation process (Willeke, 1980), (Leong, 1981).

Solid particulate can also be aerosolized by other methods. With the rotating brush method, a plug or dust cake is moved towards a rotating brush and the dust is removed from its surface and then introduced into the exposure chamber. The rate of generation will depend on the speed of the brush (Wong, 2007). With a turntable dust generator method, an aspirator which incorporates a Venturi that takes the dust from the groove of a rotating turntable is used. The rate of generation depends on the width of the groove and the speed of the turntable (Willeke, 1980), (Reist & Taylor, 2000).

When the test material is in a liquid, it can be aerosolized by nebulization. Air is pushed at high pressure through a nozzle which induces the test material in liquid form to move into the air stream. The jet causes the test material to be impacted upon a surface and the liquid is broken in small aerosol droplets. The aerosol moves out of the nebulizer and the large droplets are returned to the reservoir of the test material (Wong, 2007). Another way to generate aerosols from liquids is using spinning disc atomizers. In this type of generator, the liquid test material is introduced in the center of a spinning disc.

The liquid moves from the center to the edge of the disc as a film and the liquid is aerosolized. The main aerosols generated by spinning disc generators are monodisperse (Lippmann & Albert, 1967), (Willeke, 1980).

Vibrating orifice aerosol generators can also create monodisperse aerosols from liquid test material (Chen & Huang, 1998). The liquid is passed at a certain flowrate through a vibrating orifice which will induce the liquid to break into droplets. If the frequency of the vibrations of the orifice and flowrate of test material are constant, the aerosols generated should have the same size (Willeke, 1980).

For some inhalation studies, the test material is in a vapor form. Vapors can be generated either by transport into the chamber, or by heating the test material, and either continuous or incremental generation of vapors is possible (Hammad et al. 1985), (Wong, 2007).

The generation of gases is straightforward. Compressed gas cylinders can be obtained commercially. The concentration of the gas in the chamber will depend on the flow of the gas into the chamber. The concentration at equilibrium in parts per million for gases can be calculated using Equation 4.

$$C = (KQ_A/Q_S)\ 10^6 \qquad (4)$$

Where "Q_A" is the flowrate of the test gas, and "Q_S" is the total flowrate of gas and air in the system. "K" is the mixing factor described earlier. Equation 4 is derived from Equation 1 and the units are in parts per million. The value of "$(KQ_A/Q_S)\ 10^6$" can be used in Equation 2 for the determination of gas concentration at any time during the

inhalation challenge study (Leong, 1981).

Measurement of Test Material

Gravimetric analysis methods are the most common type of analysis used for the estimation of concentration of solid particles. For personal exposure estimation, the gravimetric analysis can be performed following the National Institute for Occupational Safety and Health (NIOSH) 500 (NIOSH, 1994) and 600 methods (NIOSH, 1998). Both methods require a 37 mm cassette with PVC filters. The main difference is the addition of a cyclone for the NIOSH 600 method. The cyclone attachment is used when the respirable fraction of the dust cloud is of interest. Inhalable samplers are used when the particle size of interest is the inhalable fraction (Hinds, 1999). The main obstacle with the gravimetric analysis in inhalation challenge studies is that the average concentration of the test material is known after the conclusion of the inhalation challenge study (Willeke, 1980). For better control of the exposure in the chamber, knowing the concentration while conducting the experiment is important. Direct reading instruments provide this capability. Direct reading instruments for gases and vapors use gas chromatography or infrared spectrophotometry methodologies, which can provide an almost instantaneous, or real time, reading of the concentration (Wong, 2007). Direct reading instruments for aerosols are also available. Several techniques are used for the determination of the mass in near real time. One method of direct reading for solid particles is using piezoelectric quartz crystals. These crystals are induced to oscillate at a certain frequency. When the solid aerosols are impacted or precipitated on these crystals, it results in a change of frequency (Hinds, 1999). Another similar method of detection

that takes into consideration the change in frequency is the tapered element oscillating microbalance (TEOM). A filter and filter holder are placed at the end of a vibrating element. Similar to the piezoelectric quartz crystals principle, when particles are collected on the filter, a change in the frequency of the oscillation of the element is induced (Wong, 2007).

Another direct reading method for the determination of solid aerosol concentration is the beta gauge method. This method requires the material be collected on a filter located between a beta source and a beta detector. The mass collected on the filter attenuates the radiation emitted by the beta source and captured by the beta detector. The difference in the amount of radiation from the beta source and the amount of radiation captured by the beta detector is proportional to the mass collected on the filter (Hinds, 1999), (Hammad & Weill, 1980).

Aerosols can be also measured by their light scattering characteristics. Instruments that use this mechanism produce a light beam that is scattered when the beam hits particles. The measurement of the amount of particles will depend on the intensity of the light scatter detected (Vincent, 2007).

Limitations of This Study

This characterization and evaluation of performance applies only to this whole-body human exposure chamber. Data obtained from this research are representative only of the test material, system flowrates, rates of generation used, and the chamber itself. These data do not apply to other test materials or inhalation challenge systems. If this exposure chamber is used with other test materials, the procedures for the determination

of the concentrations inside of the chamber, as explained in this report, should be performed prior to conducting any inhalation challenge study.

This study does not evaluate the potential adverse health effects associated with the inhalation of fly ash and carbon dioxide. No animal or human inhalation challenge studies were conducted during this research.

Chapter Two

Literature Review

The natures of nose-only and head-only exposure chambers are described previously. This review will focus only on literature regarding whole-body human exposure chambers for inhalation challenge studies.

Inhalation Challenge Systems

Hammad, Rando and Abdel-Kader (1985) created a 5 m^3 stainless steel exposure chamber for human inhalation challenge studies. The test agent was introduced through a narrow duct where it was mixed with the intake air of the system. The agents used in this study were toluene diisocyanate, formaldehyde and diiphenylmethane diisocyanate. The test material and air mixture was then passed through air splitters and screens for an even air pattern and therefore even distribution of the test material inside the inhalation challenge system. To avoid leakages of the contaminants from the chamber to the room, the system was maintained at negative pressure. The chamber had an airlock for the introduction of subjects to the system. This airlock allowed subjects to enter and exit the system when the test material's concentrations were at equilibrium. Hammad et al. reported that average toxicant concentrations in the chamber were close to the target concentrations with a difference less than 10%. Formaldehyde concentrations ranged from 0.3 ppm to 3.0 ppm as required by the inhalation challenge study protocol. Toluene diisocyanate or TDI concentrations averaged 20 ppb. It was noted that it took 60 minutes

to reach TDI concentration at equilibrium due to the time required for the walls of the chamber to saturate. Diiphenylmethane diisocyanate or MDI vapor was introduced to the chamber but due to its low vapor pressure, a condensation process took place resulting in the MDI being in an aerosol form inside the chamber. MDI average concentration was 26.7 µg/cm at the moment of injection of the test material. When increasing the injection three-fold, the average concentration inside the camber was 69 µg/cm. The particle size distribution reported for MDI had a count median diameter of 1.1 µm and a geometric standard deviation of 1.22.

In 1994, Jönsson, Welinder and Sharping developed an 8 m^3 stainless steel exposure chamber for exposures to anhydride atmospheres. The test material was generated by using test tubes filled with the substance in liquid form. Twenty five tubes, with permeation membranes of silicon rubber, were placed in a box or chamber that was submerged in a solution of water and polyethylene glycol. The temperature of the bath ranged from 45° to 110° C. Air was passed over the top of the box where the tubes were placed and this moved the gaseous material in to the chamber. Once the test material entered the exposure chamber, a fan was used for continuous mixing of the test atmosphere. Monitoring of the concentration inside the chamber was done with infrared spectroscopy equipment. Amberlite XAD-2 sorbent tubes were used as the media for the collection of the hexahydrophalic anhydride. Jönsson et. al. reported a correlation of 0.99 between the concentrations obtained with the sorbent tubes and the infrared spectroscopy equipment. During this study, the researchers intended to generate three different concentrations of the test material: 10, 40 and 80 µg/m^3. When the target concentration in the chamber was 10 µg/m^3, the researchers were able to obtain the intended

concentration with a coefficient of variation of 15%. At a target concentration of 40 $\mu g/m^3$, the concentration obtained was 37 $\mu g/m^3$ with a coefficient of variation of 5%. At 80 $\mu g/m^3$, they were able to obtain 81 $\mu g/m^3$ with a coefficient of variation of 6%

Like the Hammad et al. system, an airlock was also included in the design of an inhalation system built by C. Lidén, Lundgren, Share, G. Lidén, Tornlings and Krantz (1998). The stainless steel chamber had a volume of 5.7 m^3. The test material used for the evaluation of performance was wheat flour and it was dispersed using a rotating brush. Wheat flour was used as a test material because the researchers were interested in researching baker's asthma, dermatitis and urticaria. Krypton 85 source was used for the neutralization of the aerosols generated. To avoid contaminants other than the test material entering the chamber, the exposure chamber was maintained at positive pressure when compared to the airlock. Lidén et al. reported average concentrations of 5 mg/m^3 with the possibility of reaching concentration as high as 12 mg/m^3. Using Casella cyclones, it was determined that 6% to 12% of the total dust concentration was in the respirable fraction. Spatial variation reported was 15% and the temporal variation was in the range of 7% to 11%. Particle size distributions reported had modes between 6 µm to 10 µm and for fine particles and 50 µm for coarse particles. It was noted that a Wright Dust Feeder could be used for the dispersion of wheat flour but the particle size distribution was altered by this method of generation. No data were shown comparing the particle size distributions obtained with both methods of aerosol generation.

In 2006, this inhalation challenge system was moved to another location, while maintaining the same configuration described before. The characterization of the chamber was done with wheat flour, pinewood dust and glove powder. Direct readings

were made with light scattering instruments. IOM samplers and Casella cyclones were used for determination of inhalable and respirable fractions. Open face cassettes 37 mm in diameter were used for the determination of total dust. Cellulose filters were used in all samplers. Lundreng et al. reported achieving total dust concentrations of 5 mg/m^3 for wheat flour, 6 mg/m^3 for pinewood and glove powder. The coefficient of variation ranged from 6% to 10%. Respirable fraction dust concentrations achieved were 0.5 mg/m^3 for one type of wheat flour and 0.3 mg/m^3 for the other two types of wheat flour used. Respirable fraction concentration for pinewood was 1 mg/m^3 and 0.6 mg/m^3 for glove powder. The coefficient of variation for pinewood was 9% and was 10% for glove powder. Wheat flour variation of concentration ranged from 21% to 36%. Variability for inhalable dust was not reported due to the low number of measurements taken.

Taylor, Parker, Reist, Brian, Boehlecke and Robert (2000) developed a whole-body human exposure chamber for endotoxin exposure. The 6.5 m^3 chamber was made out of cinder block and Plexiglass with glass windows. For the creation of the endotoxin aerosol, the bacterium was adhered to microcrystalline lattice particles. The particles were heated prior the adhesion process to avoid organic contamination. During this adhesion process, the bacterium, in this case *E. agglomerans*, went through a sonication process and then was suspended in acetone solution. Then cellulose was added to the mix and it was heated. By using light microscopy, the researchers reported that the count median diameter of the preparation of cellulose particles with the endotoxin was 3.6 µm. When using a cascade impactor, they reported that the particle size distribution had a mass median diameter of 1.6 µm and a geometric standard deviation of 2.06. Mass median diameter and count median diameter reported by Taylor et al., are surprising

since the count median diameter is usually lower than the mass median diameter (Hinds, 1999). It is unknown if these were the actual results or the result of a typographical error. For the dispersion of the aerosols, a modified turntable dust feeder was used. The modification consisted of using a cylinder open on both ends instead of a cone as the reservoir of the particles. This cylinder was placed on the turntable, and it rotated freely at the same time the turntable rotated. This allowed filling the turntable groove uniformly. Prior to each run, the walls of the chamber were coated with a layer of dust to induce quick stabilization of the dust dispersed in the chamber. This conditioning of the walls was performed by dispersing the aerosols onto the clean walls for two hours. A light scattering dust monitor was used for the evaluation of the performance of the chamber while conducting the dust generation. The researchers wanted to measure endotoxin concentrations using different types of filters. The filters used were mixed cellulose ester, PVC, gelatin, zeta and glass fibers. For the simulation of an office environment, the flow rate of the system was 50 CFM which provided 11.5 air changes per hour. Taylor et al. found low variation of dust concentration within each type of filter, although no coefficient of variation was reported. The researchers also reported that dust concentrations achieved ranged from 250 $\mu g/m^3$ to 400 $\mu g/m^3$.

In 2005 Suarez et al. developed a whole-body exposure chamber to study effects of environmental tobacco smoke. The 10 m^3exposure chamber was constructed from stainless steel. It also had a 5 m^3 mixing room prior the chamber for the introduction of the test material. This material was moved from the mixing room to the exposure chamber through a vertical plenum that was installed between the mixing room and the exposure chamber. Propionic acid was used as the vapor test material and cigarette

smoke was used as the particulate test material. For the generation of the vapors, air was passed over the top of the liquid acid in the mixing room, and actual cigarette smokers were used for the generation of particulates. Like most inhalation challenge systems mentioned previously, the chamber was maintained at negative pressure to avoid test material leakage. A direct reading infrared spectrometer was used for the evaluation of the vapor concentrations and a tapered element oscillating microbalance was used for the evaluation of the particulates in the exposure chamber. Suarez et al. reported that the chamber was capable of reaching the target vapor concentration of 10 ppm in 20 minutes and maintaining the concentration over a period of 60 minutes. The target particulate concentration was 100 $\mu g/m^3$. This concentration was achieved by maintaining the concentrations of the smoke in the chamber between 75 $\mu g/m^3$ and 150 $\mu g/m^3$. The target concentration was achieved 90% to 95% of the time during the generation. The variability of concentration of the test material throughout the exposure chamber was not reported.

Sällsten et al. (2006) described an inhalation challenge system for wood smoke exposures. The chamber had a volume of 128 m^3 and had the capability to expose 10 subjects at the same time. The exposure chamber was covered with Teflon impregnated glass fiber fabric. The smoke was generated by burning hardwood and softwood that had been dried over a year in a cast iron stove placed outside the chamber. The smoke generated was mixed with clean air prior entering the chamber. Subjects were exposed for four hours. Continuous monitoring of the smoke inside the chamber was made with a tapered element oscillating microbalance (TEOM 1400). $PM_{2.5}$ and PM_1 measurements were obtained with stationary and personal air sampling equipment. Particle size

distributions were determined with an electric low-pressure impactor. Carbon monoxide and carbon dioxide were measured using infrared instrumentation. Nitrous oxides were measured with chemiluminescence instruments. Sällsten et al. noted no difference in concentrations between $PM_{2.5}$ and PM_1 data. Data from the electric low pressure impactor indicated that almost all particles sampled had a diameter less than one micrometer. During two sessions, the particle size distribution of the first session had a geometric mean diameter of 0.042 µm with a geometric standard deviation of 1.7. For the second session, the geometric mean diameter was 0.112 µm with a geometric standard deviation of 1.4. Average particle concentrations were in the range of 240 $\mu g/m^3$ to 280 $\mu g/m^3$. The researchers also reported concentrations of volatile organic compounds obtained in both sessions as descriptive data. None of the volatile organic compounds had target concentrations reached during the generation of smoke.

In 2008; Eduard et al., developed a whole-body exposure chamber for inhalation challenge studies using aerosols. The exposure chamber had a total volume of 16 m^3 made out of stainless steel. Like Hammad et al. (1985) and Lidén et al. (1998), this chamber had a 2 m^3 pre-room to avoid any disturbance of the concentration when entering into the test atmosphere, and subjects would enter only when the test atmosphere had reached equilibrium. The aerosols were dispersed using a fluidized bed generator. The dust generator had the capability of removing the bigger particles with a cyclone with a cut-off diameter of 3.5 µm. Once the aerosols generated passed the cyclone, they were neutralized using a Kr-85 neutralizer. A pneumatic vibrator was added to the dust generator to avoid dust deposition between the dust generator and the cyclone and the neutralizer. The test material used in this study was fused aluminum oxide. The

concentrations of the test material inside the chamber were monitored using an optical particle counter. Also, active sampling with 25 mm diameter PVC filters was performed. Eduard et al. reported that equilibrium concentration was reached between 30 to 60 minutes after the generation was started, depending on target concentration. The concentrations of the test material measured at different positions inside of the exposure chamber were statistically different. Concentrations at the center of the chamber were higher than the concentrations in the periphery. For concentrations lower than the 1 mg/m^3, the coefficient of variation of aerosol concentration was 10% to 19%. When concentrations in the chamber were higher than 1 mg/m^3, the researchers reported a coefficient of variation of 4% to 6%. Concentrations could be maintained for more than 1 hour after reaching a stable concentration. Particle size distribution determined by the particle counter showed a volume mean diameter of 5.7 µm without the cyclone. With the cyclone attached to the generator, the volume mean diameter was 2.9 µm.

Other reports about utilization and performance of inhalation challenge system were also discussed by Green and Thomas (1986), Sandström et. al. (1989), Rudell et. al. (1996), Sunblad et. al. (2004), Schiffman et. al, (2005) and Toumainen et. al. (2006).

Mixing Factors

The concentration's buildup and decay equations are derived from the general dilution ventilation equation. This general equation is used to estimate the concentration in a room, if the rate of generation and the air flow through the system are maintained constant and if there is complete mixing. Equation 5 considers the conservation of mass of air contaminant in a specific workroom (Jaylock, 1998).

$$VdC = Gdt - QC/K\ dt \quad (5)$$

In other words, the concentration in the room is equal to the rate of generation of the contaminant minus the removal rate (NIOSH, 1992). “V”, “C”, “G”, “t”, “Q” and “K” are the same as discussed previously. If all variables are maintained constant and there is an interest to see what the effect of time is; Equation 5 can be rearranged as shown in Equation 6.

$$\int_{Ct1}^{Ct2} dC/(G - QC/K) = 1/V \int_{t1}^{t2} dt \quad (6)$$

Where Ct1 is the concentration at time 1 or at “t1” and Ct2 is the concentration at time 2 or at “t2”. Equation 6 can be solved as shown in Equation 7 (NIOSH, 1992).

$$\ln\left[\left(G - \frac{QCt2}{K}\right) \Big/ \left(G - \frac{QCt1}{K}\right)\right] = -Q/KV\ (t) \quad (7)$$

Equation 7 can be rearranged as shown in Equation 8 by using exponentials.

$$Ct2 = KG/Q\ (1 - e^{-QT/KV}) + Ct1\ (e^{-QT/KV}) \quad (8)$$

The mixing factor or variable “K” is associated with the airflow of the system

(NIOSH, 1992), (Esmen, 1978), (Feigley, 2006). It is defined as the proportion of the flow of the system that actually mixes with the test material, also known as "Q effective" (American Conference of Governmental Industrial Hygienists, 2004).

Often in the literature, the mixing factor can also be found described by the variable "m". The relation between the variables "m" and "K" can be seen in Equation 9.

$$m = 1/K \tag{9}$$

Ideal or perfect mixing is usually defined with a value of 1 for "K" or "m" (Popendorf, 2006). Mixing factor values can range from m_i 0.1 to 1 or, K from 1 to 10, depending which variable is being used.

In inhalation challenge systems, the mixing factor will affect the concentration level at equilibrium and the time of buildup and decay of concentration. If mixing factor is defined with the "K" variable, the higher values of "K" will result in high concentrations of the test material and longer buildup and decay of concentration. On the other hand, better mixing or low "K" values would mean lower concentrations but faster buildup and decay of concentration times (NIOSH 1992). Determination of mixing factor values have been of interest in the past, for example in 1978, Esmen reported that the estimation of the mixing factor in enclosed ventilated rooms using the general buildup and decay equations cannot be applied to all situations. He explained that the estimation of the mixing factor could be difficult when the air in the room is recirculated and there are multiple sources of the contaminant (Esmen, 1978). In 1980, Ishizu tried to estimate the mixing factors values by measuring cigarette smoke concentrations in a room with

recirculated air. He found that the mixing factor "m" values for his experiment ranged from 0.3 to 0.6.

In 1992, Bowes, Mason and Corn tried to determine the mixing properties of a tracer gas in a confined space. They measured the concentration at the inlet and outlet of the room. Flow rates, volume of the room and times were measured. Then, they divided the buildup and decay of concentration in half lives. For the purposes of the experiment, the half live was defined as the time that it would take for the test material to reach half the concentration. Several half lives were obtained during the buildup and decay of the concentration. Bowes et al., determined theoretical half lives using the buildup and decay equations and compared them with the half lives obtained with the measured data. They defined the mixing factor as the ratio between the experimental half live obtained from the data and the theoretical half live from the model. They reported mixing factors values or "K" values from 0.27 to 1.52.

The mixing factor is also considered as the sum of several factors that can affect the mixing of the test material (Feigley et al., 2002). Some of the factors that can affect the mixing are the design of the exposure chamber, how well is the mixing of the test material before entering the exposure chamber, leakages in the exposure chamber, position of inlets and outlets of air and particle size distribution of the test material (McClellan & Henderson, 1995), (Bowes et. al., 1992). When the mixing factor is used as a "safety" factor for the protection of workers, the toxicity of the material is also taken in consideration (American Conference of Governmental Industrial Hygienists, 2004).

Tapered Element Oscillating Microbalance

Patashnick and Rupprecht developed a direct reading instrument for measurement of particulate mass concentrations. The instrument consists of an oscillating tapered element with a filter. When particulates are collected by the filter, it will produce a change in the frequency of oscillation. The relationship between the mass deposited and the frequency of the oscillating tapered element is presented in Equation 10 (Patashnick & Rupprecht, 2004).

$$\text{mass} = K_o\,(1/f^2_b - 1/f^2_a) \qquad (10)$$

Where "K_o" is the constant specific to the oscillating element and the variable "f" represents the frequency. The instrument measures the mass collected every two seconds. The total mass measured is then integrated in an exponential smoothing to obtain a total smooth mass concentration. This concentration displayed by the instrument for every minute is actually a moving average of 10 minutes (Patashnick & Rupprecht, 2004). The filter is kept at 50° C to avoid any effects by the humidity. The instrument can be modified to measure particles within different particle size ranges. The most common particle size range measured with the Tapered Element Oscillating Microbalance or TEOM is the PM_{10}. The PM_{10} or particulate matter 10 defined by the Environmental Protection Agency as "inhalable coarse particles" that have particle size between 2.5 µm and 10 µm. PM_{10} particle size should not be confused with inhalable fraction defined by the American Conference of Governmental Industrial Hygienists or ACGIH. The ACGIH defines the inhalable fraction as particles with a cutoff diameter or

d_{50} of 100 µm. The thoracic fraction and respirable fraction has a d_{50} of 10 µm and 4 µm respectively (ACGIH, 2009).

Comparisons have been made between the mass concentrations obtained with the TEOM and concentrations obtained by gravimetric analysis. In 1999, Salter and Parsons compared the results of 100 days data obtained with the TEOM and the Partisol, a gravimetric monitor. The filter of the Partisol monitor was weighted every 4 days. Salter et al. reported that TEOM results were lower than the concentrations obtained by the Partisol monitor. They also reported that at low concentrations; the data between the instruments were in agreement and as the particulate concentration increased, the difference between the results of the instruments also increased. The difference between the TEOM and the gravimetric analysis was attributed to the possible volatilization of particulate matter in the filter of the TEOM (Salter et al., 1999). In 2008, Wanjura, Shaw, Parnell, Lacey and Capareda reported similar results when comparing the TEOM with gravimetric total suspended particulate or TSP samplers.

In 1999, Soutar, Watt, Cherrie and Seaton compared the TEOM with the Institute for Occupational Medicine or IOM area sampler. This sampler was designed for the gravimetric analysis of the inhalable size fraction. Comparisons were performed in six separate occasions and each occasion had four consecutive 24 hour sampling times. Souter et al. reported that results obtained with the IOM area sampler were higher than the results obtained with the TEOM. He also reported high correlation between the results of the TEOM and IOM area samplers.

Personal Inhalable Fraction Samplers

Several samplers have been designed to meet the inhalable fraction sampling criteria including the IOM personal sampler and the button inhalable sampler. The IOM personal sampler was the first inhalable sampler available and is the closest that matches the inhability curve (Vincent, 2007). In 2000, Aizenberg, Grinshpum, Willeke, Smith and Baron described the performance of a button personal inhalable sampler and compared it with the IOM personal sampler using a manikin in a wind tunnel. Aizenberg et al. reported that the sampling efficiency of the button sampler was not affected by the direction of the wind and the coefficient of variation was found to be equal to or better than the other samplers evaluated. Similar results were found by Linnainmaa et al. (2008) where in laboratory and field tests, they found agreement between the results obtained by the IOM sampler and the button inhalable sampler.

Quartz Crystal Microbalance Cascade Impactor

The quartz crystal microbalance cascade impactor or QCM cascade impactor that provides direct reading particle size distributions. Each stage contains two piezoelectric quartz crystals. One of the crystals is the sensing crystal which is placed beneath the nozzle exist for impaction of the particles. The second crystal or reference crystal does not collect particles and it is used as the control (California Measurements, 2004). The relation between the mass and change in frequency of the crystals can be seen in Equation 11.

$$\Delta mass = - (1.4 \times 10^{-9}) \Delta f \qquad (11)$$

Where 1.4×10^{-9} is the average mass sensitivity of the electrode when particles are impacted or deposited across the electrode. In 1984, Farichild and Whet performed an evaluation of a QCM cascade impactor. They concluded that the accuracy of the particle size distributions would be affected by the high percentage of wall losses of the cascade impactor. They also concluded that the impactor should not be used for particles with an aerodynamic diameter higher than12 µm because the calculated effective cutoff aerodynamic diameter for stages 1 and 2 were different from the actual effective cutoff aerodynamic diameters. The high wall losses were also found by Horton, Ball and Mitchell. In 1992, Horton et al., evaluated the PC-2 QCM cascade impactor with monodisperse aerosols. They found particle bouncing between stages to be insignificant. It was also found that the particle collection at the first stage and possibly the second stage were not optimal. Mass median aerodynamic diameters or MMAD obtained with the QCM cascade impactor were comparable with the MMAD obtained with the Andersen cascade impactor.

In 1999, Tzou compared the QCM cascade impactor with the Andersen cascade impactor using metered-dose inhalers aerosols or MDI. He also found that the MMAD obtained with the QCM and Andersen cascade impactor were in agreement.

Health Effects

Health effects of particulates have been widely discussed in the literature. Studies linking particulate matter and different lung conditions have been published elsewhere (Curtis et al., 2006). The Environmental Protection Agency or EPA has a National Ambient Air Quality Standard of 150 µg/m^3 for PM_{10} for an average time of 24 hours and

15 µg/m^3 for $PM_{2.5}$. The Occupational Safety and Health Administration had established a permissible exposure limit or PEL of 15 mg/m^3 for total particulate not otherwise regulated and 5 mg/m^3 for respirable particulate not otherwise regulated. Both limits are based on a time weighted average of 8 hours. Main health effects associated with carbon dioxide are narcotic effects and asphyxiation. The ACGIH recommends a threshold limit value or TLV of 5000 ppm for a time weighted average of 8 hours and a short term TLV of 30,000 ppm (ACGIH, 2010).

Chapter Three

Methodology

Components of Whole-Body Human Exposure Chamber

A whole-body human exposure chamber was developed for inhalation challenge studies for gases and particulates. The Plexiglas chamber has a volume of 2.13 m^3 and it is operated at negative pressure to avoid any contaminants leaking to the room. The core components of the system include high efficiency particulate air filters, orifice meters, a mixing chamber and an air blower.

1. High Efficiency Particulate Air Filters

Three High Efficiency Particulate Air or HEPA filters are used for filtration of air. The first HEPA filter is placed at the intake of air of the inhalation challenge system to avoid particles from the intake air mixing with the test material and entering the chamber. A second HEPA filter is placed after the exposure chamber to prevent test material in the solid state entering and damaging the air blower. When the scrapper of the dust generator engages with the reservoir of the test material, an initial cloud develops creating a peak of the concentration of the test material in the chamber. To avoid this, the exposure chamber is bypassed during the first 15 minutes of the dust generation. The bypass is connected to a high flow pump with the third HEPA filter connected inline.

2. Orifice Meters

Air flow measurements of the exposure chamber are performed with orifice meters. An orifice meter is installed after the HEPA filter at the intake of the system and a second is installed before the air blower. For the construction of the orifice meters, a one and a half inch diameter PVC duct was used. A plate with an orifice one inch in diameter is drilled in it. The orifice is inserted inside the PVC pipe. When the air passes through the orifice, it will force the air flow to contract, at the Vena Contracta; and induce a pressure change after the orifice. A Magnehelic gauge is connected to the orifice meter to measure the differential pressure before and after the orifice (ACGIH, 2001). The difference in pressure before and after the orifice is related to the air flow rate. The orifice meters are calibrated with a Micro-Pitot tube (Hinds, 1999), and using Equation 12.

$$V = (4005\sqrt{VP})*0.9 \quad (12)$$

Once the average velocity was known, Equation 13 was used for the determination of the air flow rate passing through the orifice meter.

$$Q = VA \quad (13)$$

Where "V" is the average velocity and "A" is the area of the duct. The difference in pressure measured by the magnehelic gauge was then correlated to the air flow rate passing through the orifice meter. Calibration curve data for both orifice meters can be

found in Appendix A.

3. Dust Mixing Chamber

The dust mixing chamber was constructed from PVC and has a volume of 5 liters.

4. Air Blower

A Spiral^{TM} SL4P2 air blower manufactured by Ametek Industrial Products is used for moving air in the inhalation challenge system. It has the capacity to move up to 2 cubic meters of air per minute. An air bypass before the air blower is installed between the second orifice meter and the blower. The bypass is used to regulate the flow rate of air in the system. Air from the blower is exhausted through a laboratory fume hood.

Gas Generation and Measurement

As explained previously, the generation of gases is straightforward. In this research, carbon dioxide is used as a tracer gas (Greinert et al., 1992). A schematic diagram of the exposure chamber when use for gas generation is shown in Figure 1. The arrows represent the direction the flow.

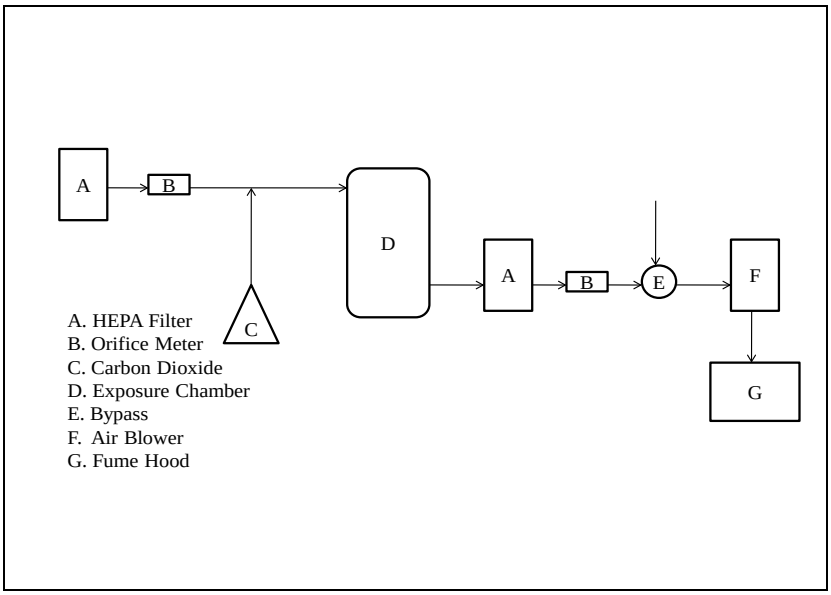

Figure 1. Schematic Diagram of Inhalation System for Gases.

1. Carbon Dioxide

Carbon dioxide (CO_2) was used as a tracer gas because of its relative low toxicity, ease of detection and low cost. Because CO_2 is present in the atmosphere, background concentrations were taken into consideration during gas injection into the exposure chamber. Measurements of CO_2 were made using Metrosonic aq-5000 infrared instruments. Calibration of the instruments was performed before its use.

2. Dry Gas Meter

A dry gas meter was used for the measurement of the volume of CO_2 injected into the chamber. Calculation of CO_2 flowrates can be found in A.

Generation and Measurement of Particulates

Fly ash was used as the test material for the generation and evaluation of the behavior of particulates in the exposure chamber. A schematic diagram of the exposure chamber when used for particle generation is shown in Figure 2. The arrows represent the direction the flow.

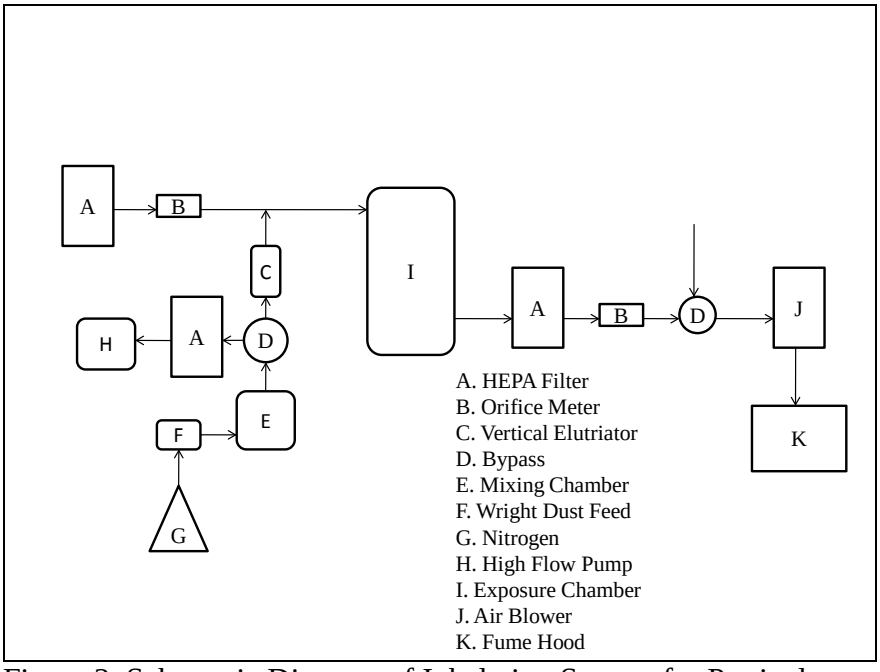

Figure 2. Schematic Diagram of Inhalation System for Particulates.

The components used for the generation and measurement of particles are listed below:

1. *Fly Ash*

Fly ash was used as the test material for the characterization and evaluation of performance of the exposure chamber. The fly ash was donated by a local power plant.

2. Dust Generator

A Wright Dust Feeder (BGI Incorporated, Waltham, Massachusetts), was used for the generation of the fly ash dust cloud. The principle of this generator is that the dust, in this case, the fly ash; is packed in the dust generator's chamber as a "cake" and then it is scrapped (Wright, 1950). For the characterization of the exposure chamber, the Wright Dust Feeder was set at the following RPM settings: 0.2, 0.4, 0.8 and 1.6. Dry nitrogen from a compressed cylinder was used to carry the fly ash from the dust generator to the inhalation challenge system.

3. Nitrogen

Compressed nitrogen was used for the movement of fly ash from the dust generator into the system. The flowrate of the gas was measured using a calibrated rotameter. The flowrate of the nitrogen was maintained at 8.4 L/min for all the generation procedures of aerosols. See Appendix C for calibration of rotameter.

4. Vertical Elutriator

A vertical elutriator is used for the separation of large and agglomerated fly ash particles (Walton, 1954). It is constructed from a Plexiglas pipe with an inside diameter of 7.3 inches (18.5 cm). The aerosol dust cloud passing through the elutriator is directed towards the chamber through a PVC tubing 1.5 inches in diameter. The diameter of the largest particles of fly ash theoretically passing through the elutriator and entering the exposure chamber is determined using Stoke's Law, as shown in Equation 14.

$$d = \sqrt{\frac{(V)(18)(\eta)}{(\rho)(g)}} \qquad (14)$$

Where "d" is the diameter of the particle, "V" is the velocity of the gas passing through the elutriator, "η" is the viscosity of the gas, "ρ" is the density of the particle and "g" is the acceleration due to gravity. The theoretical diameter of the fly ash particles passing the elutriator and entering to the system is 8 μm or lower. See Appendix D for the calculation for the determination of the aerodynamic diameter of the fly ash passing the vertical elutriator.

5. *Tapered Element Oscillating Microbalance*

A TEOM 1400ab was used for the continuous measurement of particle concentration inside of the exposure chamber. The concentration displayed by the instrument is an average of 10 minutes that updates every 2 seconds. The results are reported in $\mu g/m^3$. See Appendix E for the data obtained from the TEOM for each generation of particulates.

6. *QCM Cascade Impactor*

Determination of particle size distributions at different rates of generation was made using a QCM Cascade Impactor, Model PC-2. This instrument was manufactured by California Measurements. The cascade impactor has 10 stages and the cut-points aerodynamic diameter of the instrument has a range from 0.1 μm to > 35 μm. Since the first stage of the impactor doesn't have pre-impactor, the cut-point of the first stage is >

35 µm. The first stage of the instrument was used as the pre-impactor of the cascade impactor because as stated previously, the theoretical diameter of the fly ash particles entering into the chamber is 8 µm or lower.

7. Air Sampling Pumps

MSA Escort Elf pumps and SKC AirChek XR5000 were used along with SKC aluminum cyclones for the determination of particulate concentration in the respirable fraction. Calibrations of the air pumps are shown in Appendix F.

8. Filters

PVC filters 37 mm and 25 mm in diameter and 5 µm pore size were used for determination of total dust concentrations, and inhalable and respirable fraction concentrations inside the chamber. Determination of total dust and respirable fraction concentrations was performed by using 37 mm open-face cassettes and the inhalable fraction concentration was determined using a SKC Button Aerosol Sampler with 25 mm PVC filters. The cassettes and the sampler were connected to a copper plenum, and the plenum was connected to a high flow air pump. A syringe needle was used as a critical orifice for the regulation of air passing through each filter. High flow air pumps were used for calibration of the 37 mm cassettes and the button sampler. This calibration can be seen in Appendix G.

Procedures for the generation of gases and particulates in the whole-body human exposure chamber are shown in Appendix I and Appendix H respectively.

Particle Size Distribution

Determination of particle size distributions was determined using the QCM cascade impactor. Five consecutive particle size distributions were obtained at each RPM setting in order to obtain an average particle size distribution for each RPM setting. The average particle size distributions of each RPM setting were compared between each other.

Distribution of Concentration in the Chamber

Twelve PVC filters 37 mm in diameter placed in open face cassettes were used for the determination of dust concentration across the exposure chamber. The filters were placed four and a half feet above the floor of the chamber. Five consecutive generations of fly ash were made. Each generation or run lasted 5 hours to ensure enough dust was collected on the filters. Blank filters were left overnight in the weighing room for the filters to reach equilibrium with environmental conditions of the room. After collection of the samples, the filters were left overnight in the same weighing room before the final weights were obtained. Gravimetric analysis was made following the NIOSH Analytical Method 0500. For the purpose of comparison, twelve dust filters were divided into three patterns. The first pattern was for comparison between four rows of the filters. The second pattern was for comparison of two rows at the front and two rows at the back the chamber. The third pattern was for comparison between three groups that represent left, middle and right side of the exposure chamber. See Figures 23, 24 and 25.

Concentration of Fly Ash

As stated previously, a vertical elutriator was used for the removal of large particles of fly ash. As a result not all the test material dispersed by the Wright Dust Feeder is introduced to the exposure chamber. It is therefore not possible to determine the rate of generation before the test material is measured inside the chamber. To describe the concentration in the chamber at different rates of generation, a correlation was obtained between the four different revolutions per minute (RPM) settings of the dust generator and the concentration obtained inside the chamber. The RPM settings used were 0.2, 0.4, 0.8 and 1.6. For each RPM setting, 5 consecutive dust generations were made and each run lasted 60 minutes. The concentration of the test material during each run was determined with the TEOM. An average profile of the dust concentration was obtained at each RPM setting.

Studies reported in the literature showed that there is a difference between the results of the TEOM and gravimetric analysis (Salter et al., 1999), (Soutar et al., 1999). Therefore, determination of total, inhalable and respirable dust fraction concentrations, were made in comparison with the TEOM. 37 mm open face cassettes, SKC button sampler and SKC cyclones were used for total, inhalable and respirable dust.

Operation of the Inhalation Challenge System

1. Gas Generation

Gaseous test material is introduced into the system by injecting the gas to the ductwork entering the chamber. Gas flowrates were measured before its introduction. Atmospheric background concentrations of carbon dioxide were obtained before

introducing it to the chamber. A step by step procedure for the generation of gases can be found in Appendix H.

2. Particle Generation

A step by step procedure for the generation of particulates can be found in Appendix I. During the generation of particles, three major pitfalls may arise: difference in concentrations inside the exposure chamber due to the condition of fly ash, incorrect positioning of the dust generator's scraper in relation to the fly ash plug and the initial dust cloud pulse when starting the generation of fly ash.

Fly ash was oven dried at 200 °C over 12 hours (overnight) period before using it for dust generation. This drying process minimizes the effects of moisture in the fly ash. If the fly ash is not dried, it will agglomerate and fly ash agglomerates will be excluded by the vertical elutriator, resulting in a lower dust concentration inside the chamber. The difference between dried and undried fly ash concentrations is show in Figure 3.

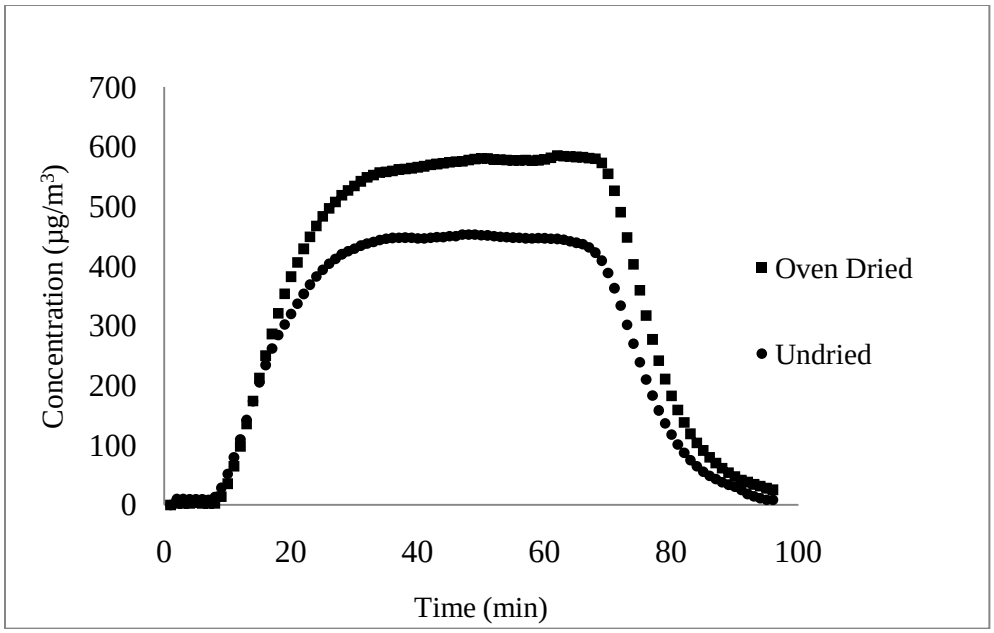

Figure 3. Comparison between Oven Dried and Undried Fly Ash.

After the drying process, the fly ash was compacted in the dust chamber of the Wright Dust Feeder with a 2-ton Ann Arbor press. Using the press ensures consistency of the compaction of the fly ash among dust generation runs. Once the dust is compacted, it is important that the dust plug is close to the scraper of the Wright Dust Feeder. As explained before, if the scraper is not in contact with the compacted fly ash, a slow build up of concentration is reflected in the chamber as shown in Figure 4.

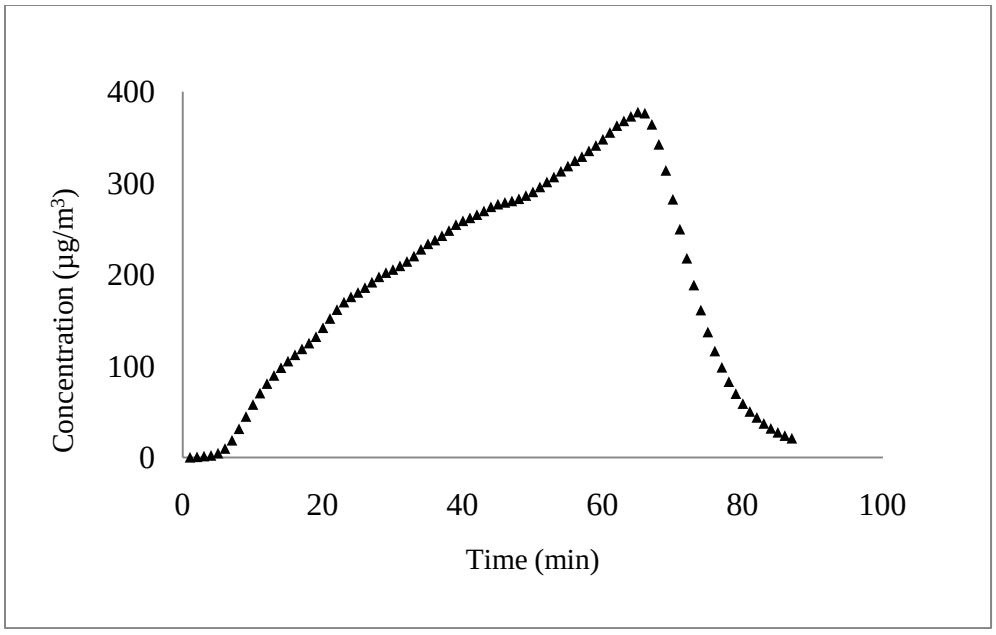

Figure 4. Effect of Incorrect Positioning of Scraper of Dust Generator.

Using the press will also prevent the effects of improper packing of fly ash. If the fly ash is not compacted properly, some portions of the fly ash plug could fall. This will result in an initial pulse cloud of test material entering the chamber and affecting the dust concentration profile as shown in Figure 5.

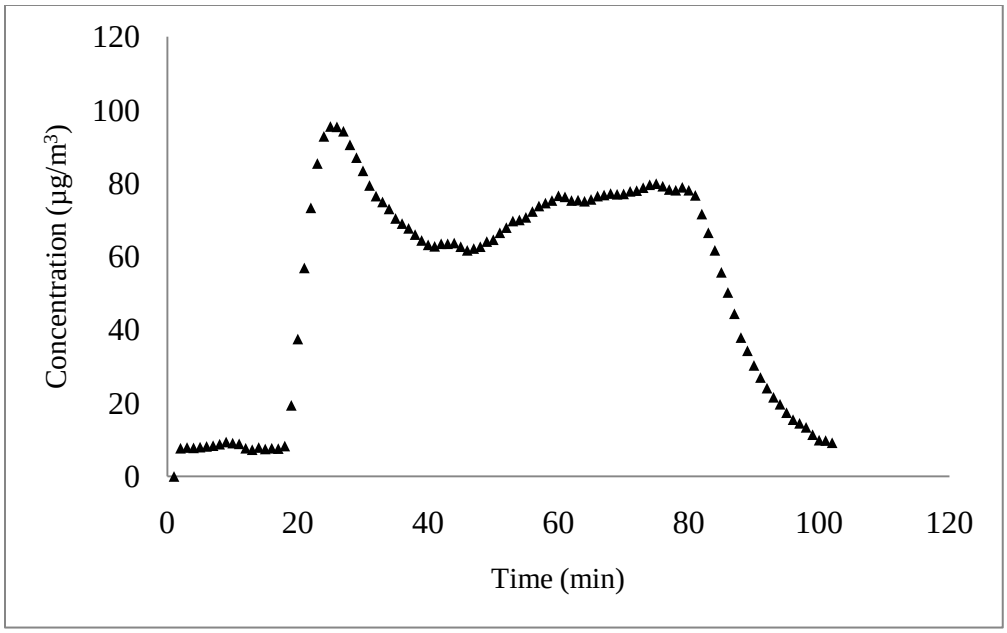

Figure 5. Effect of Initial Dust Cloud within Dust Concentration Profile.

To avoid this initial pulse going inside the chamber, the Wright Dust Feeder is started for 15 minutes bypassing the chamber as depicted in Figure 2. This ensures that the dust generator's scraper is engaging the fly ash plug and the initial pulse do not affects the fly ash concentration profile in the exposure chamber.

Statistical Analysis

1. Evenness of Concentration

Twelve open face 37 mm cassettes with PVC filters were positioned inside the exposure chamber for determination of concentration levels across the chamber. The data for this comparison were obtained by dividing the mass collected at each filter by the volume of air that passed through that specific filter. This computation provides a concentration value in units of micrograms per cubic meter of air for each position inside the exposure chamber. As described earlier, dust concentration values were gathered in

different group pattern for comparison. Wilcoxon rank-sum test was used as the statistical test for this comparison. This non parametric test was selected because of low sample size and normality of distribution could not be assumed. Multiple comparisons were made for each pattern and a Bonferoni correction was performed depending on the amount of comparisons made. This statistical procedure tested the following hypothesis:

H_O: There are no statistical differences between the dust concentration levels of the different group patterns inside the exposure chamber.

H_A: There are statistical differences between the dust concentration levels of the different group patterns inside the exposure chamber.

2. Particle Size Distribution

Particle size distributions were obtained by using the QCM cascade impactor. The data for this comparison were obtained by dividing the concentration registered by the instrument at each stage by the sum of the concentrations registered at all stages. This value was then multiplied by 100 in order to obtain a percentage. Five particle size distributions were obtained at each RPM setting. The five particle size distributions were then averaged to obtain an average particle size distribution for each RPM setting. Wilcoxon rank-sum test was also used as the statistical test for this comparison because of the low sample size and the particle size distributions have a log-normal distribution. A Bonferroni correction was made for six comparisons. This statistical procedure tested the following hypothesis:

H_O: There are no statistical differences among the particle size distributions at RPM settings of the dust generator 0.2, 0.4, 0.8 and 1.6.

H_A: There are statistical differences among the particle size distributions at RPM settings of the dust generator 0.2, 0.4, 0.8 and 1.6

Chapter Four

Results

Orifice Meter Calibration

The orifice meters in the inhalation challenge system are identified as OM-1A and OM-1B. OM-1A is located after the HEPA filter at the intake of the system and OM-1B is located before the air blower. Calibration curves for both orifice meters are shown in Figure 6 and Figure 7.

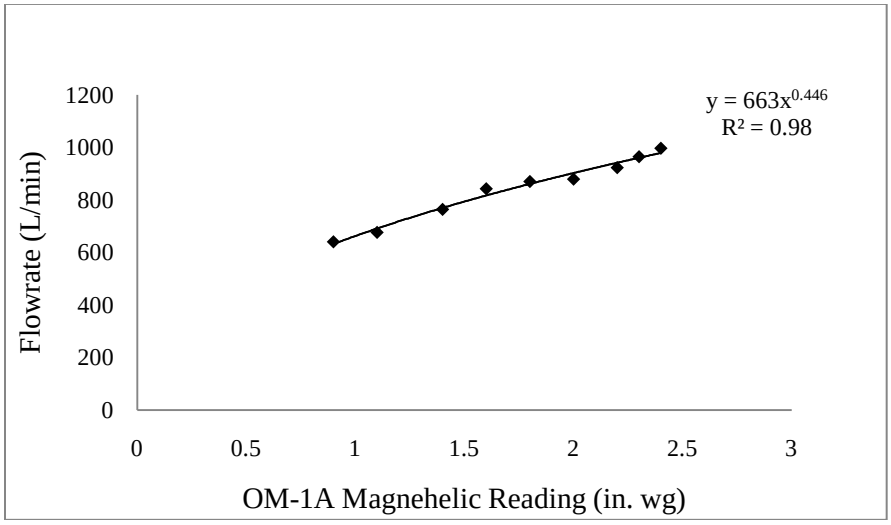

Figure 6. Calibration Curve of Orifice Meter OM-1A.

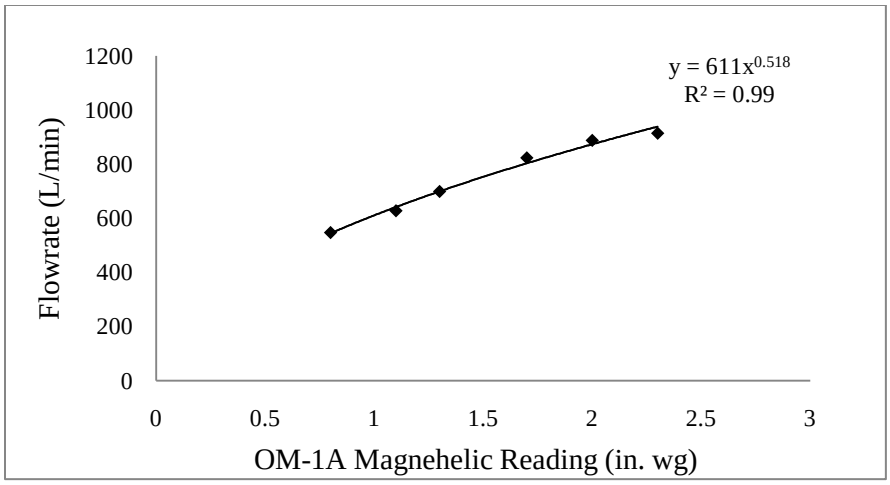

Figure 7. Calibration Curve of Orifice Meter OM-1B.

The calculated equation of the power regression for OM-1A and OM-1B are shown in Equations 15 and 16 respectively, where Y is the flowrate calculated using Equations 12 and 13. X is the reading of the individual magnehelic gauge connected to each orifice meter.

$$\text{Flowrate} = 663\ (\text{Mangahelic Reading})^{0.446} \quad (15)$$

$$\text{Flowrate} = 611\ (\text{Mangahelic Reading})^{0.518} \quad (16)$$

The calculated coefficient of determination or R^2 for both regression lines was higher than 0.98.

Buildup and Decay Profiles of Carbon Dioxide

Buildup and decay patterns were measured at the top and bottom of the exposure chamber. Four consecutive buildup and decay patterns at a rate of generation of 4.8 L/min are shown in Figure 8.

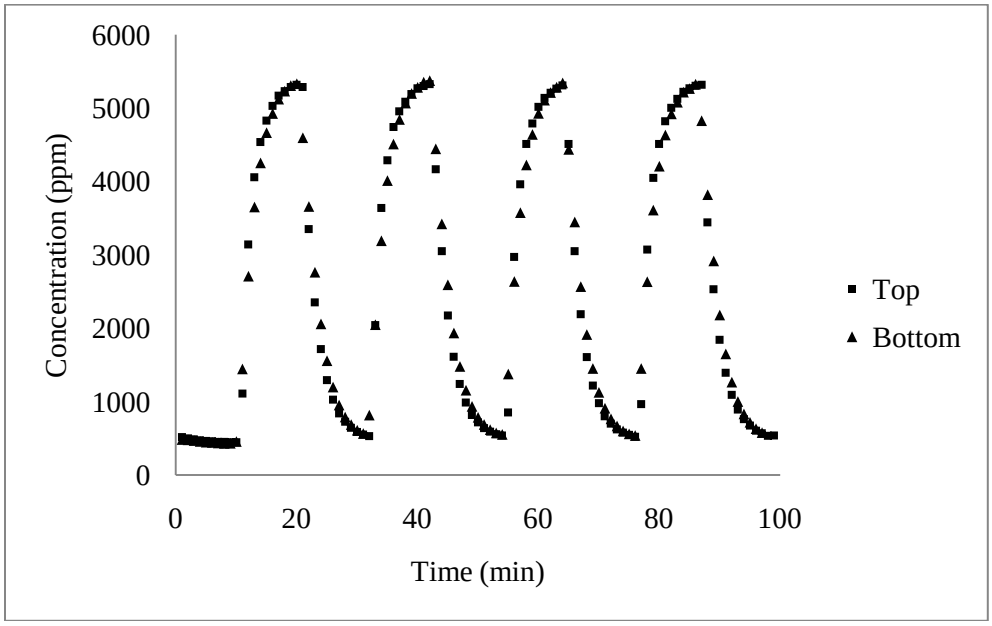

Figure 8. CO_2 Buildup and Decay Patterns at the Top and Bottom of Exposure Chamber.

Buildup and decay pattern of carbon dioxide were measured on the front, back, left and right side in the exposure chamber. Two CO_2 infrared monitors were mounted on a stand for the concentration measurement during gas generation. During the first generation, the instruments measured carbon dioxide concentration in the front and back side of the chamber. After the first generation, the stand was rotated, in a way that the monitors were located in the left and right side of the exposure chamber. Once the instruments were in the desired place, the generation was started. Evenness of carbon dioxide concentration inside the exposure chamber is shown in Figure 9 at a rate of generation of 4 L/min.

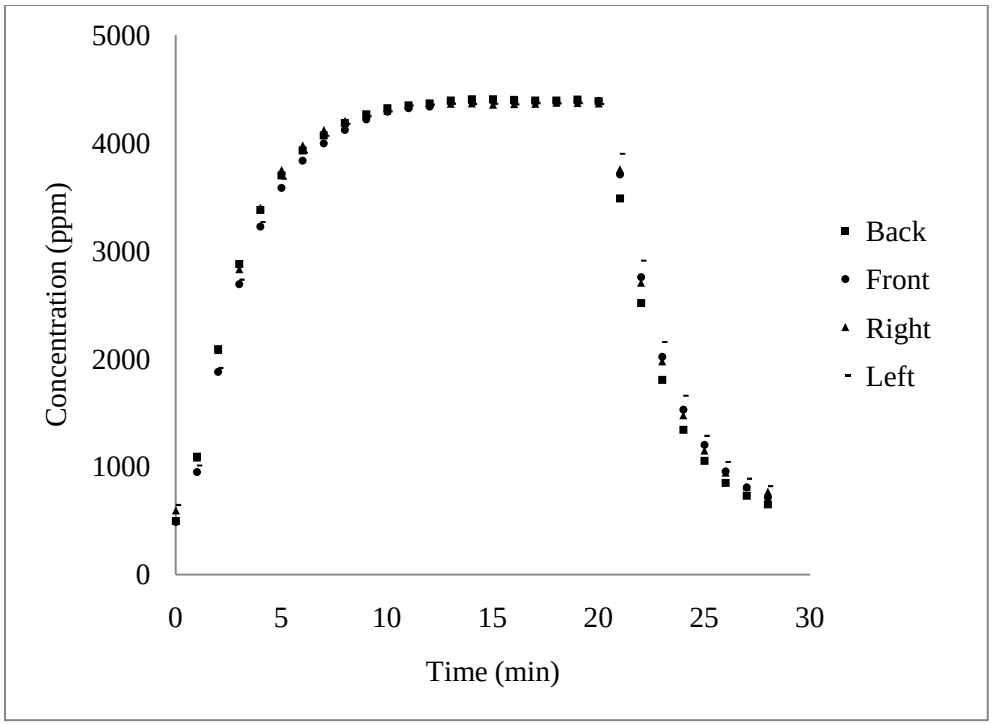

Figure 9. Evenness of Concentration of Carbon Dioxide at Different Positions in the Exposure Chamber.

Concentration Profiles of Carbon Dioxide

A drygas meter was used for the measurement of carbon dioxide gas entering the chamber. Since carbon dioxide is present in the atmosphere, background CO_2 concentration was measured prior each run. The carbon dioxide buildup and decay concentrations were modeled using Equation 2 and Equation 3 respectively and applying a mixing factor value of 1. Various gas generations profiles are shown below in Figures 10-12. The generation rates and generation times varied in each case to illustrate the consistency of the generation method.

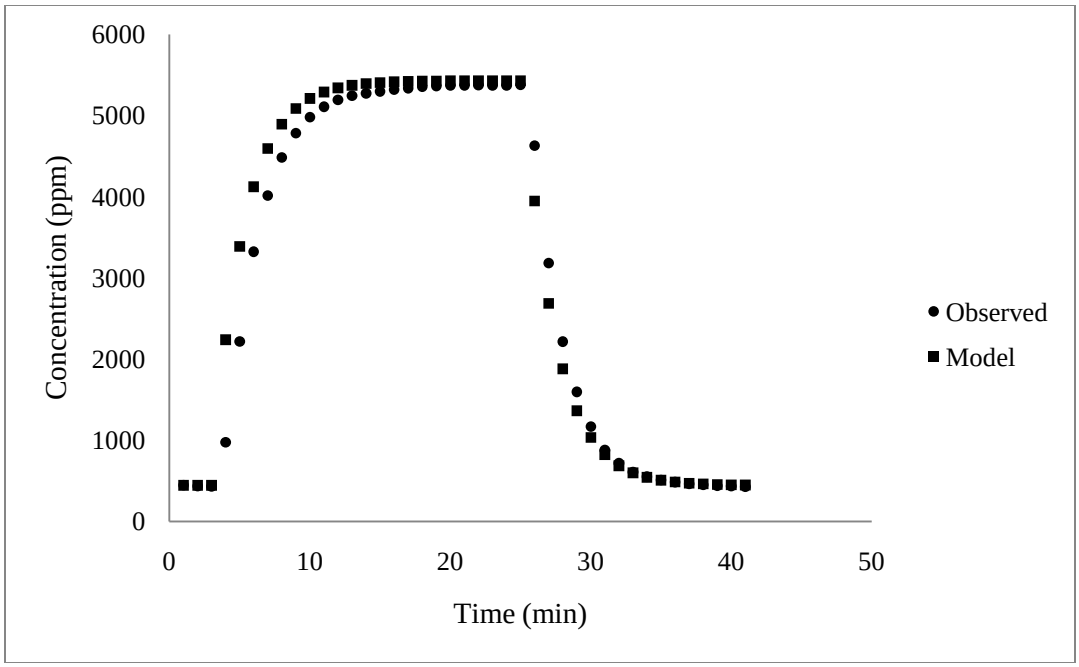

Figure 10. CO_2 Concentration and Model for Rate of Generation of 4.8 L/min. Background concentration of carbon dioxide was 444 ppm.

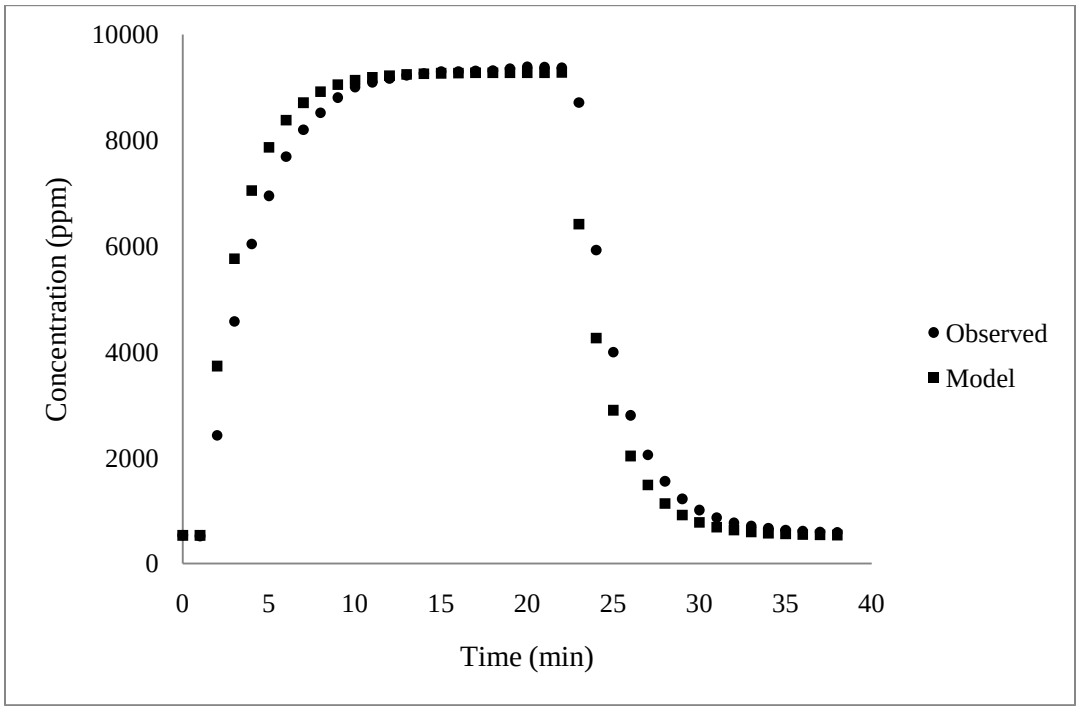

Figure 11. CO_2 Concentration and Model for Rate of Generation of 8.5 L/min. Background concentration of carbon dioxide was 532 ppm.

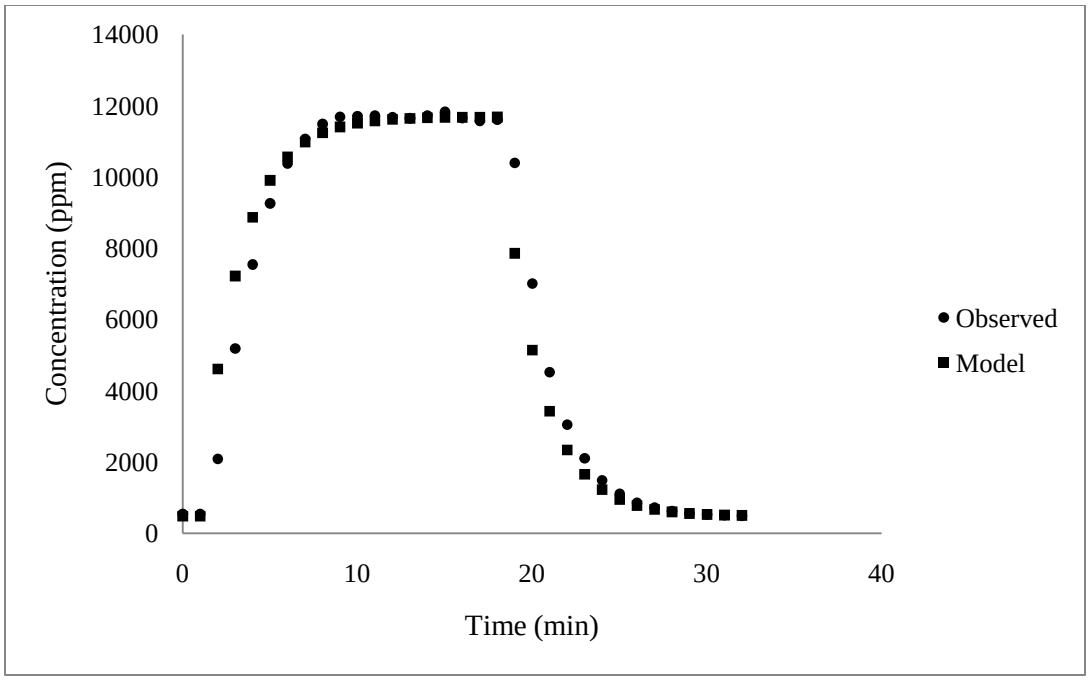

Figure 12. CO_2 Concentration and Model for Rate of Generation of 11 L/min. Background concentration of carbon dioxide was 484 ppm.

Observed and expected maximum concentrations or C_{max} for carbon dioxide are shown in Table I.

Table I. Observed and Expected C_{max} Concentrations for CO_2.

Rate of Generation (L/min)	Observed C_{max} (ppm)	Expected C_{max} (ppm)	Difference %
4.8	5,375	5,471	1.74
8.5	9,380	9,279	1.08
11	11,600	11,672	0.62

Concentration Profiles of Fly Ash Particles

The evaluation and characterization of the inhalation challenge system for particulates was made at four different RPM settings: 0.2, 0.4, 0.8 and 1.6. Five consecutive particle generations were made at each RPM setting. Concentration profiles obtained with the TEOM instrument are show below in Figure 13-16.

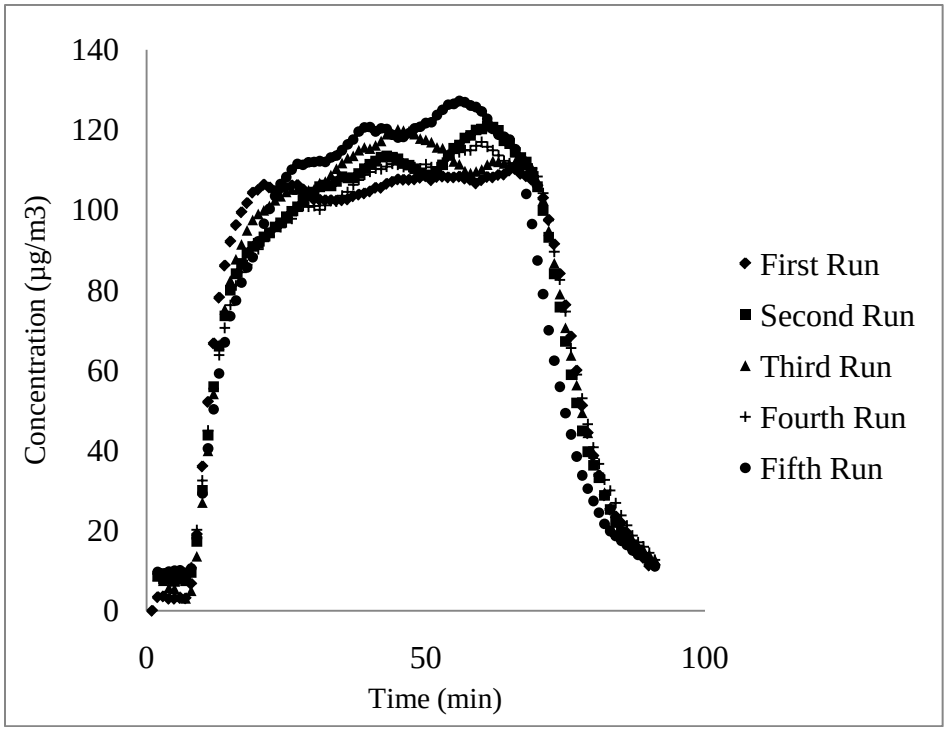

Figure 13. Particle Generation at RPM Setting 0.2. N=5. Generation time was 60 minutes.

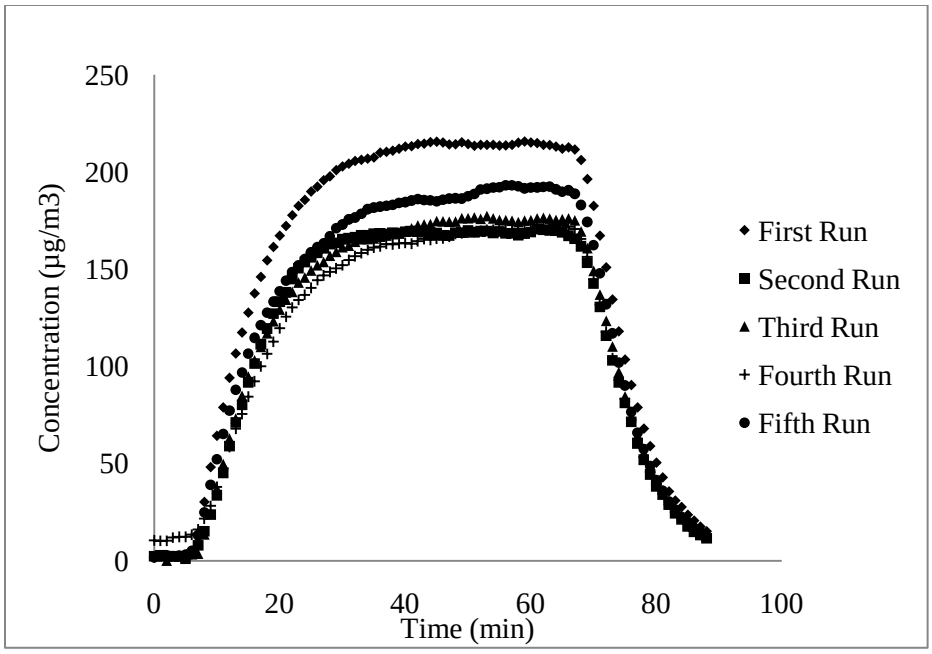

Figure 14. Particle Generation at RPM Setting 0.4. N=5. Generation time was 60 minutes.

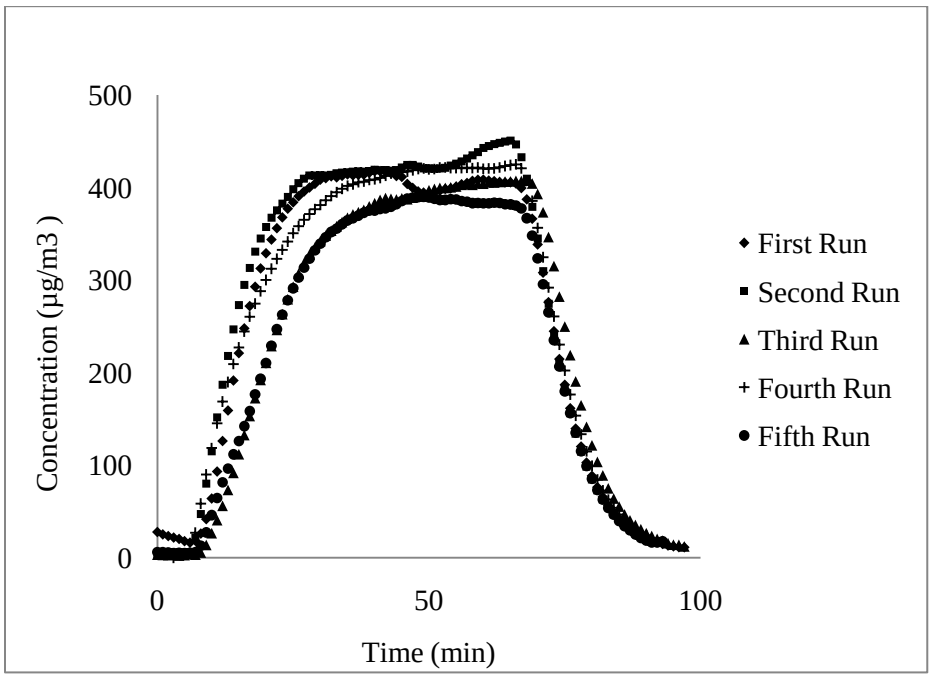

Figure 15. Particle Generation at RPM Setting 0.8. N=5. Generation time was 60 minutes.

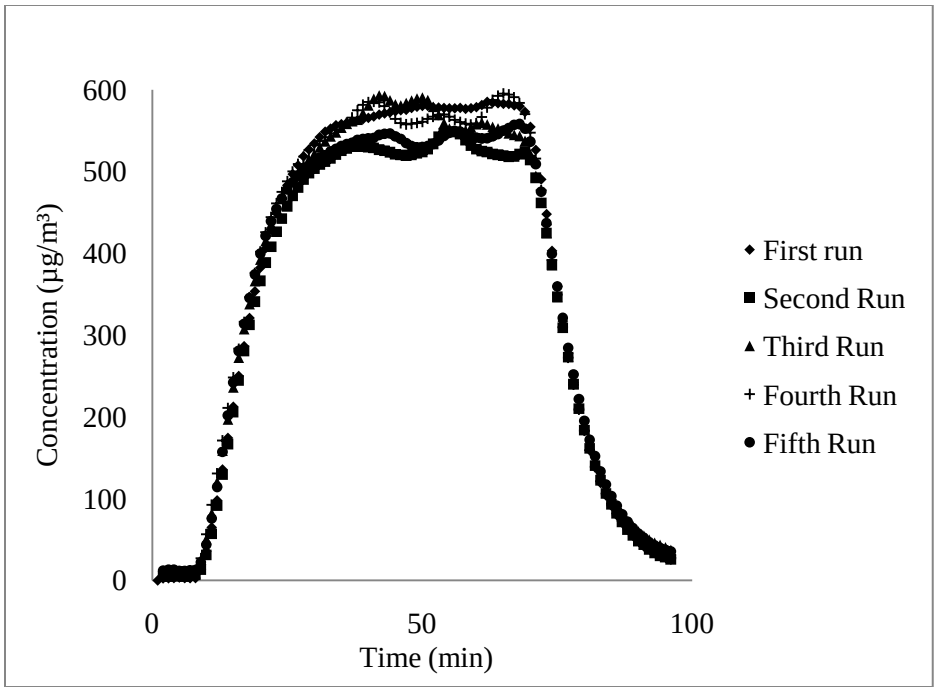

Figure 16. Particle Generation at RPM Setting 1.6. N=5. Generation time was 60 minutes.

The average concentration profile for each RPM setting is shown in Figure 17.

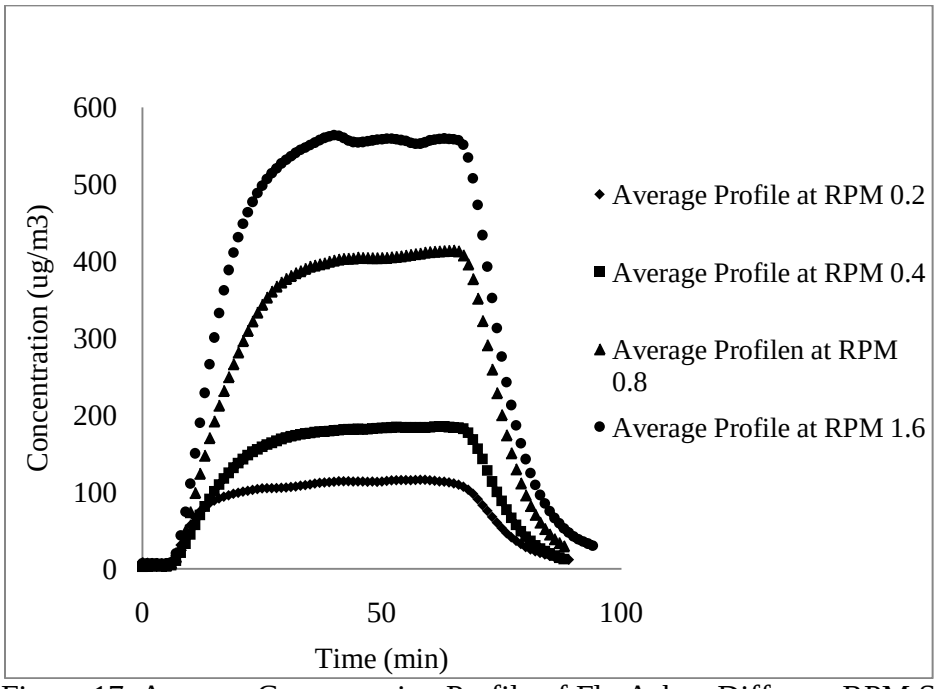

Figure 17. Average Concentration Profile of Fly Ash at Different RPM Settings.

Dust Concentration in the Chamber

Total dust concentration, inhalable and respirable fraction concentrations were determined at each RPM setting as described before. Obtained concentrations were plotted against average concentrations determined by the TEOM. The results are presented in Figures 18-20.

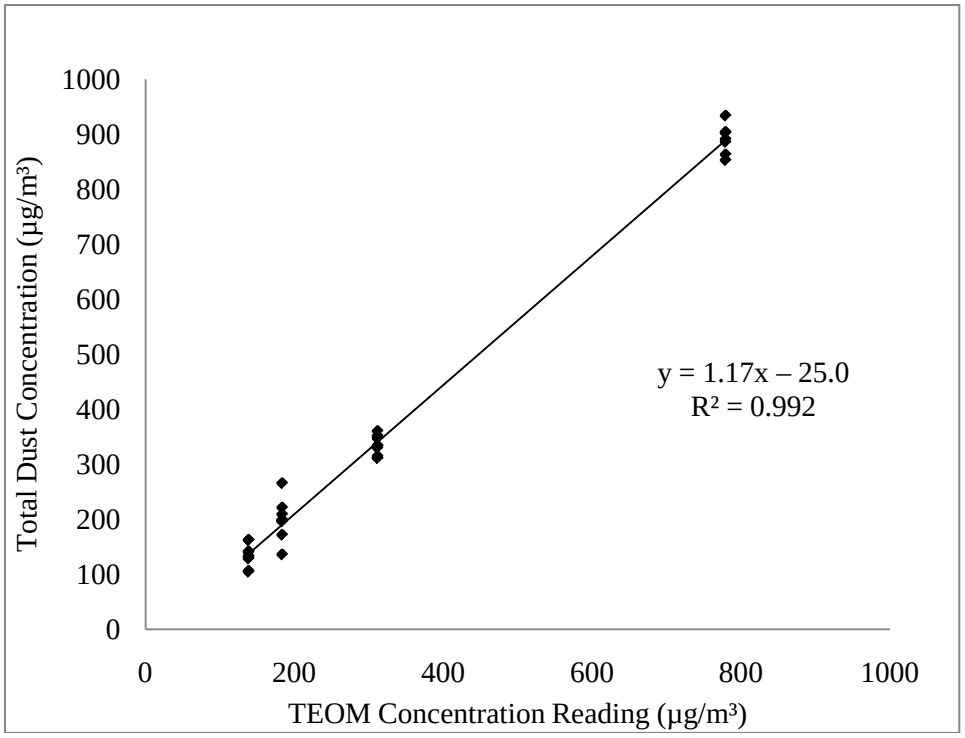

Figure18. Total Dust Concentrations vs. TEOM Average Readings at Different RPM Settings. N= 34

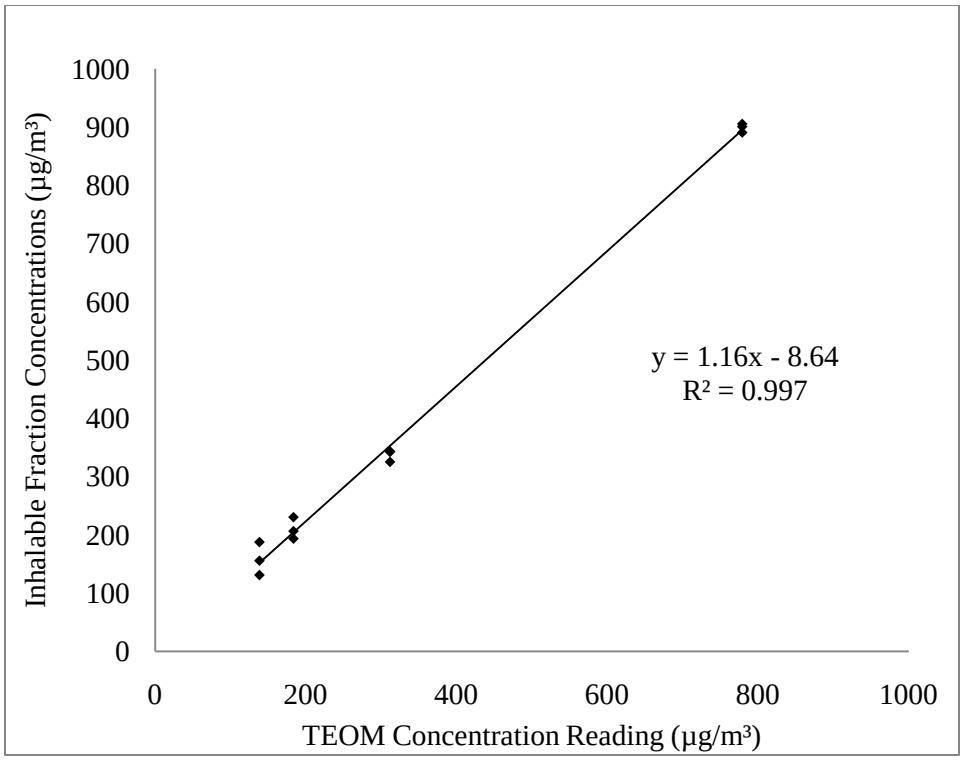

Figure19. Inhalable Fraction Concentrations vs. TEOM Average Readings at Different RPM Settings. N= 12

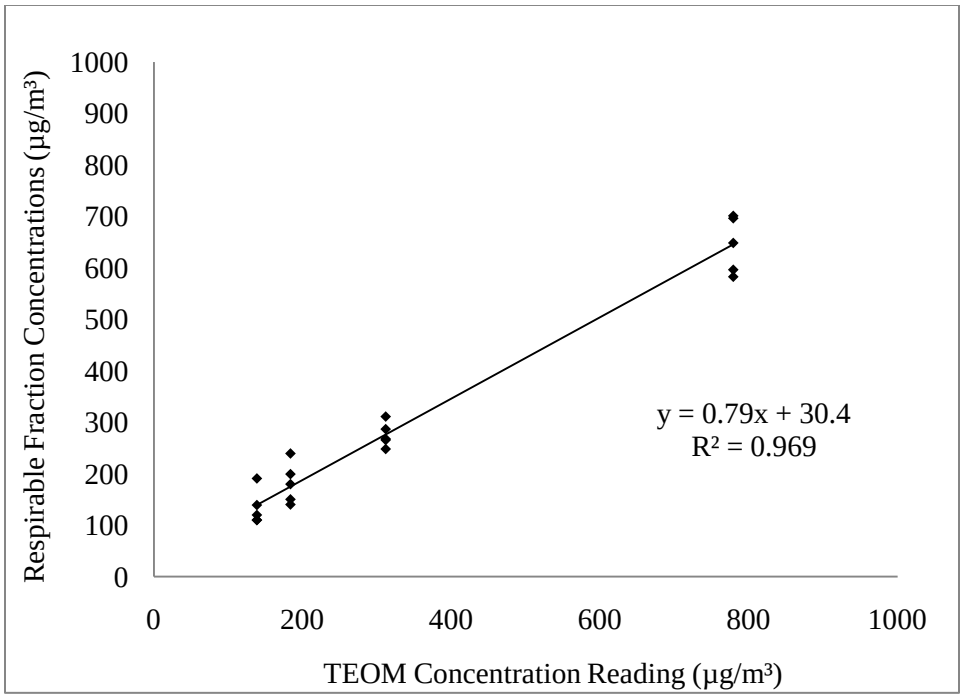

Figure 20. Respirable Fraction Concentrations vs. TEOM Average Readings at Different RPM Settings. N= 20

The calculated equation of the least-square fit regression line for total dust, inhalable and respirable fraction concentrations are shown in Equations 18, 19 and 20 respectively, where Y is the is the concentration obtained by gravimetric analysis and X is the average reading from the TEOM instrument.

Total Dust Concentration ($\mu g/m^3$) =

1.17 (TEOM) – 25.0 (17)

Inhalable Dust Concentration ($\mu g/m^3$) =

1.16 (TEOM Reading) - 8.64 (18)

Respirable Dust Concentration ($\mu g/m^3$) =

0.79 (TEOM Reading) + 30.4 (19)

The calculated coefficient of determination or R^2 for each of the three regression lines were 0.992, 0.007 and 0.969. The intercepts from Figures 18 and 19 are not statistically different from zero ($p > 0.05$). The intercept from Figure 20 is statistically different from zero ($p < 0.05$). A comparison between the total dust concentrations and the inhalable and respirable fraction concentrations can be seen in Figure 21.

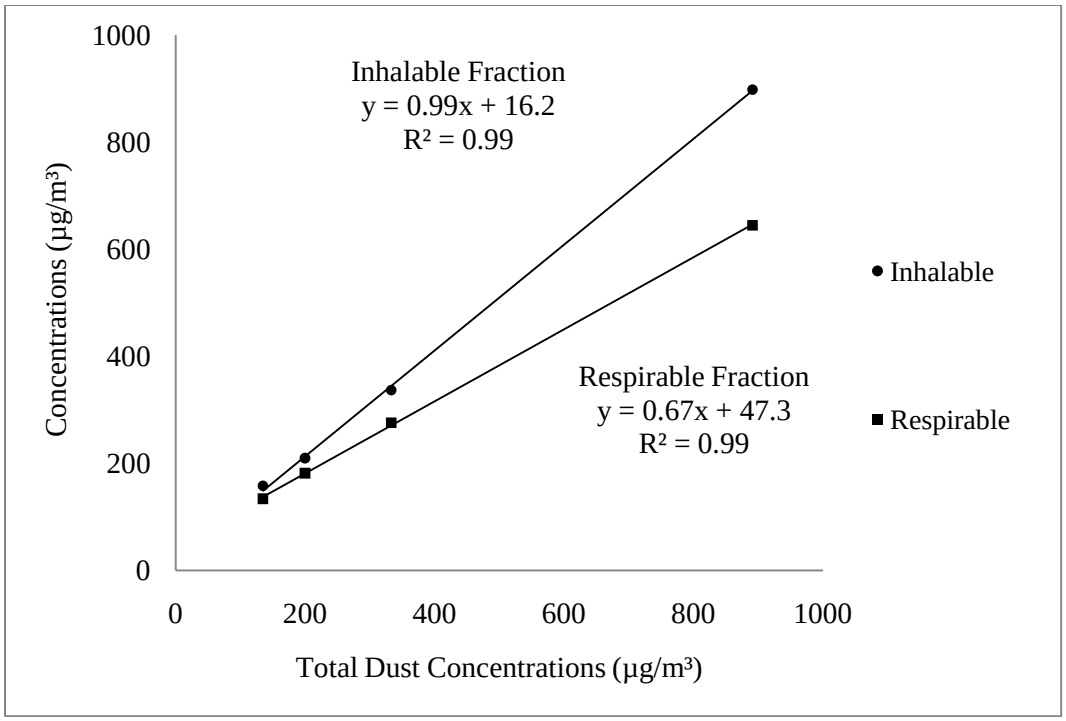

Figure 21. Regressions of Average Total Dust Concentrations vs. Inhalable and Respirable Fraction Average Dust Concentrations.

The calculated equations of the least-square regression of inhalable and respirable fraction concentrations are shown in Equations 20 and 21 respectively, where X is the total dust concentration. Y is the inhalable and respirable fraction concentration respectively.

$$\text{Inhalable Dust } (\mu g/m^3) = 0.99\,(\text{Total Dust Concentration } (\mu g/m^3)) + 16.2 \quad (20)$$

$$\text{Respirable Dust } (\mu g/m^3) = 0.67\,(\text{Total Dust Concentration } (\mu g/m^3)) + 47.3 \quad (21)$$

The calculated coefficient of determination or R^2 for both regression lines was 0.999. The intercept for the inhalable regression is not statistically different from zero ($p > 0.05$), but the intercept for the respirable fraction is significantly different from zero ($p < 0.05$). A summary of average dust concentrations obtained at different RPM settings is shown in Table II.

Table II. Average Dust Concentrations Obtained by Gravimetric Analysis.

RPM	Total Dust Concentration (µg/m³)	Inhalable Fraction Concentration (µg/m³)	Respirable Fraction Concentration (µg/m³)
0.2	135	158	134
St. Dev.	20.5	28.3	33.9
C.V.	15.2%	17.9%	25.3%
0.4	200	210	181
St. Dev.	34.9	18.7	39.8
C.V.	17.5%	8.90%	21.9%
0.8	333	337	276
St. Dev.	18.0	10.2	24.0
C.V.	5.40%	3.03%	8.70%
1.6	891	898	644
St. Dev.	27.0	7.55	54.9
C.V.	3.04%	0.84%	8.50%

Concentration Distribution across the Exposure Chamber

The concentration across the exposure chamber was determined by placing twelve open face cassettes for collection of test material. The positions of the cassettes inside of

the exposure chamber are shown in Figure 22. The evenness of distribution in the chamber was obtained by normalizing the dust concentrations at different points across the chamber during five consecutive runs. Normalization of dust concentrations was utilized to eliminate the effect of differences in dust concentrations from one run to the other. The coefficient of variation of the normalized dust concentrations inside the chamber was 7.6%. Dust concentrations are shown in Appendix J.

Back

10	11	12
7	8	9
4	5	6
1	2	3

Door

Figure 22. Schematic Diagram of Open-Face Cassettes Positioning Inside the Chamber.

For the characterization and analysis of the distribution of concentration across the exposure chamber, the concentrations obtained by the open face cassettes were grouped in three different patterns. The three different patterns are shown in Figure 23, Figure 24 and Figure 25.

Back

Group D
Group C
Group B
Group A

Door

Figure 23. Schematic Diagram of Four Open Face Cassette Pattern

Back

Group F
Group E

Door

Figure 24. Schematic Diagram of Two Open Face Cassette Pattern

Back

Group G	Group H	Group I

Door

Figure 25. Schematic Diagram of Three Open Face Cassette Pattern

Table III, IV and V show the results of the statistical analysis for the comparison of the different groups.

Table III. Statistical Comparison of Four Open Face Cassette Pattern

Comparison	*p value* >
Group A and Group B	0.967
Group A and Group C	0.886
Group A and Group D	0.622
Group B and Group C	0.967
Group B and Group D	0.742
Group C and Group D	0.869

Bonferroni correction $\alpha = 0.008$

Table IV. Statistical Comparison of Two Open Face Cassette Pattern

Comparison	*p value* >
Group E and Group F	0.702

$\alpha = 0.05$

Table V. Statistical Comparison of Three Open Face Cassette Pattern

Comparison	*p value* >
Group G and Group H	0.429
Group G and Group I	0.767
GroupH and Group I	0.335

Bonferroni correction $\alpha = 0.016$

Particle Size Distributions

A QCM cascade impactor was used for the determination of particle size distribution at different RPM settings. Five consecutive particle size distributions were obtained at each RPM setting, then an average particle size distribution was calculated for each RPM setting. The average particle size distributions were plotted on a log-probability graph for the determination of the mass median diameter or MMD and the geometric standard deviation or GSD. Average particle size distributions at different RPM settings are shown in Figure 26.

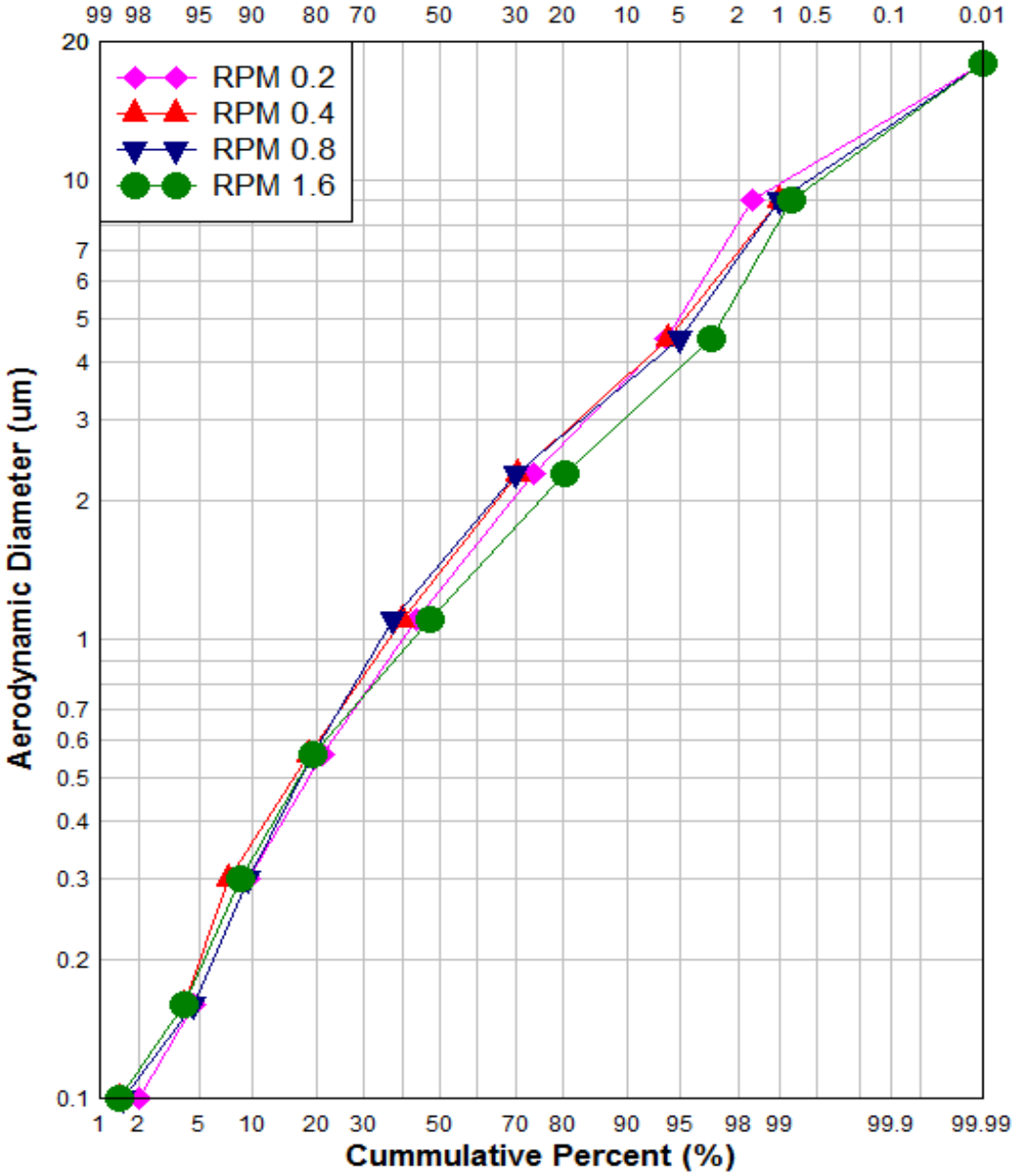

Figure 26. Average Particle Size Distributions at Different RPM Settings.

MMD and GSD for the average particle size distributions are shown in Table III.

Table VI. MMD and GSD Obtained at Each RPM Setting.

RPM	MMD (μm)	GSD
0.2	1.27	2.35
0.4	1.39	2.22
0.8	1.46	2.08
1.6	1.15	2.20

A total of 6 comparisons were made between the average particle size distributions obtained at different RPM settings. Results of statistical comparisons are shown in Table VII.

Table VII. Statistical Comparison of Particle Size Distributions

Comparison	*p value* >
RPM 0.2 and RPM 0.4	0.603
RPM 0.2 and RPM 0.8	0.861
RPM 0.2 and RPM 1.6	1.000
RPM 0.4 and RPM 0.8	1.000
RPM 0.4 and RPM 1.6	0.794
RPM 0.8 and RPM 1.6	0.794

Bonferroni correction $\alpha = 0.008$

Chapter Five

Discussion and Conclusions

Orifice Meters

Nose-only, head-only and whole-body exposure chambers have been previously described and each one has its strengths and its weaknesses. This research describes and characterizes the performance of a whole-body human exposure chamber developed at the University of South Florida. For this inhalation challenge system, the measurement of the air flow in the system is obtained with orifice meters. Figure 6 and Figure 7 show a high coefficient of determination for both calibration curves. As shown in Appendix A calibration of the orifice meters was done at different pressures: 3 inches of water, 4 inches of water and 5 inches of water to verify whether the measurements of the orifice meters (OM) were affected by changes in pressure, and they were not. All the regression equations obtained at different pressures for OM-1A and OM-1B, provide similar results. Figure 6 and Figure 7 represent the calibration curves obtained at 4 inches of water because the exposure chamber was maintained at a pressure drop of 4 inches of water during the course of this research. The flowrate in the exposure chamber was obtained by averaging the values of the two orifice meters.

Distribution of Test Material in the Chamber

Carbon dioxide was used as tracer gas because of its cost and availability of instruments for its measurement. Figure 8 shows the buildup and decay of gas concentration at the top and bottom of the chamber. The only difference between the concentrations measured by the instruments are seen when the generation of test material is started and stopped. The inhalation challenge system is designed so that the test material is introduced at the top of the chamber and will flow downward. As a result the instrument at the top of the exposure chamber will register the changes in concentration first when compared to the instrument placed at the bottom, as shown in Figure 8.

When measuring the gas concentration at different positions in the exposure chamber (right side vs. left side, front vs. back, at 2 feet above the floor), the buildup and decay profiles were similar as depicted in Figure 9. This was also found to be true when comparing dust concentrations within the chamber, as shown in Tables III, IV and V**.** Thus, the coefficient of variation of the normalized dust concentrations inside the chamber was 7.6%.

Concentration of Test Material in the Chamber

As stated previously, generation of carbon dioxide is straightforward but some issues needed to be addressed. A needle was used to maintain constant flow by physically restricting the flow. Without a needle valve a slow increase of flowrate was observed with a corresponding increase in concentration inside the chamber. Another issue that needed to be considered was the naturally occurring atmospheric carbon dioxide. The ambient the concentration of carbon dioxide was measured and the model

was adjusted for its presence

Figures 10, 11 and 12 show the carbon dioxide concentrations obtained at three different rates of generation. The model was developed by using the general buildup and decay equations previously described. The model, described previously, and the measured maximum concentrations were in close agreement for all three rates of generation with a difference ranging from 0.2% up to 1.74%. The model and the measured concentrations did differ in the buildup and decay times. All three figures show a slower buildup and decay of the observed concentrations when compared to the model. This difference most likely is due to the lag time of the instrument when measuring the concentrations.

If the concentration inside the exposure chamber was affected by incomplete mixing of the test material, not only a difference in the buildup and decay concentrations times would be seen but also a difference in the maximum concentration levels. This was observed by Ishizu (1980), who found that due to incomplete mixing, he observed higher than expected maximum concentrations levels. The flowrate in an inhalation challenge system is essential for determination of maximum concentration levels and buildup and decay concentration times. This is because the buildup and decay equations (Equations 2 and Equation3) as well as the mixing factor are dependent on the flowrate. This was observed in Figures 10, 11 and 12. Maximum concentrations were in agreement but not the buildup and decay times. It is not possible that incomplete mixing of the test material could affect the buildup and decay concentration times but not the maximum concentration levels.

Mixing characteristics of an exposure chamber can also be estimated by

comparing the measured residence time of a tracer gas with its theoretical residence time. This residence time is defined as the time that takes the test material to exit the exposure chamber once its generation had been stopped (O'Shaughnessy, 2003). For this exercise, the variable "K" represents a rate constant which takes in consideration the volume, flowrate and mixing characteristics of the chamber. The relation between "K" and the residence time is shown in Equation 22.

$$K = 1 / (\text{residence time}) \tag{22}$$

The residence time value is obtained by determine the slope of the logarithmic regression of the decay concentrations over time (O'Shaughnessy, 2003). CO_2 decay concentrations were regressed and their slopes were compared with the slopes of theoretical decay concentrations. In Figures 27 and 28, "K_m" represents the ratio of the measured and theoretical "K" values.

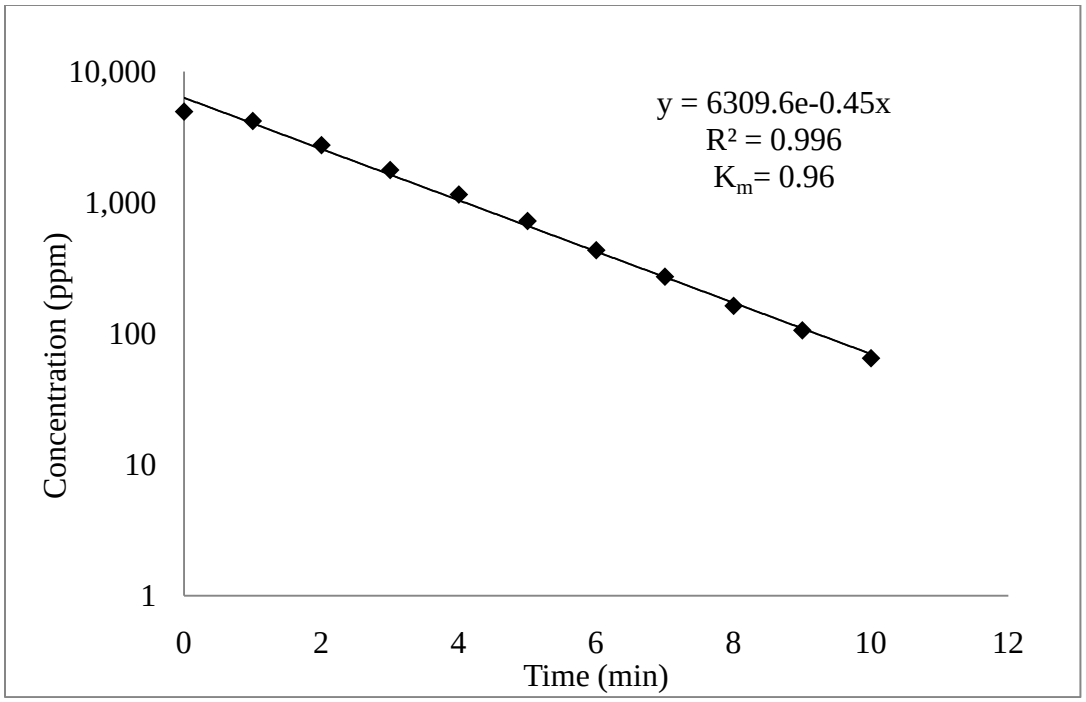

Figure 27. Concentration Decay of CO_2 for Rate of Generation of 4.8 L/min.

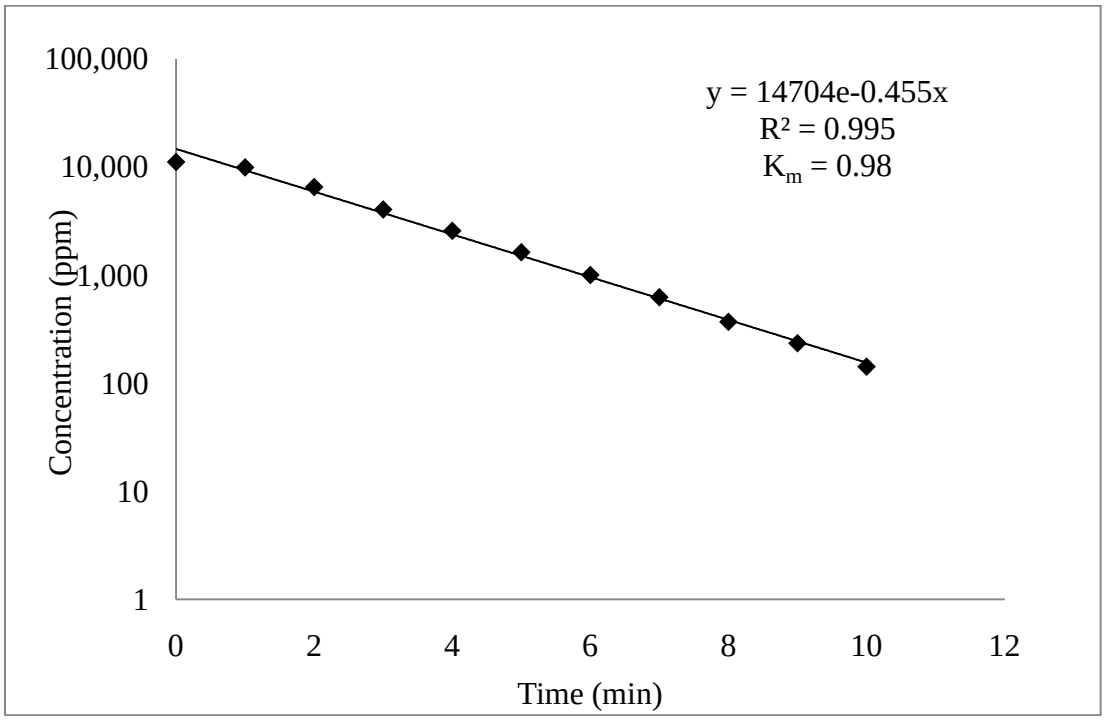

Figure 28. Concentration Decay of CO_2 for Rate of Generation of 11 L/min.

For the calculation of "K_m", the background concentration of carbon dioxide was subtracted from the observed and theoretical concentrations. The mixing values obtained for both generations demonstrate good mixing.

On the other hand, measured dust concentrations could not be compared to theoretical or expected dust concentration, as was done with carbon dioxide. Before the dust is introduced into the chamber; the dust (fly ash) it goes through a vertical elutriator and the larger particles (greater than 8 µm) are removed. This means that the true rate of particle generation is unknown. The rate of generation can be calculated from the concentrations measured. An example of the model with a mixing factor value of 1 and the average profile of dust concentration at RPM 1.6 is shown in Figure 27. An apparent rate of generation can be estimated from Figures 13-16 and from the correlation between the dust concentrations and the RPM settings

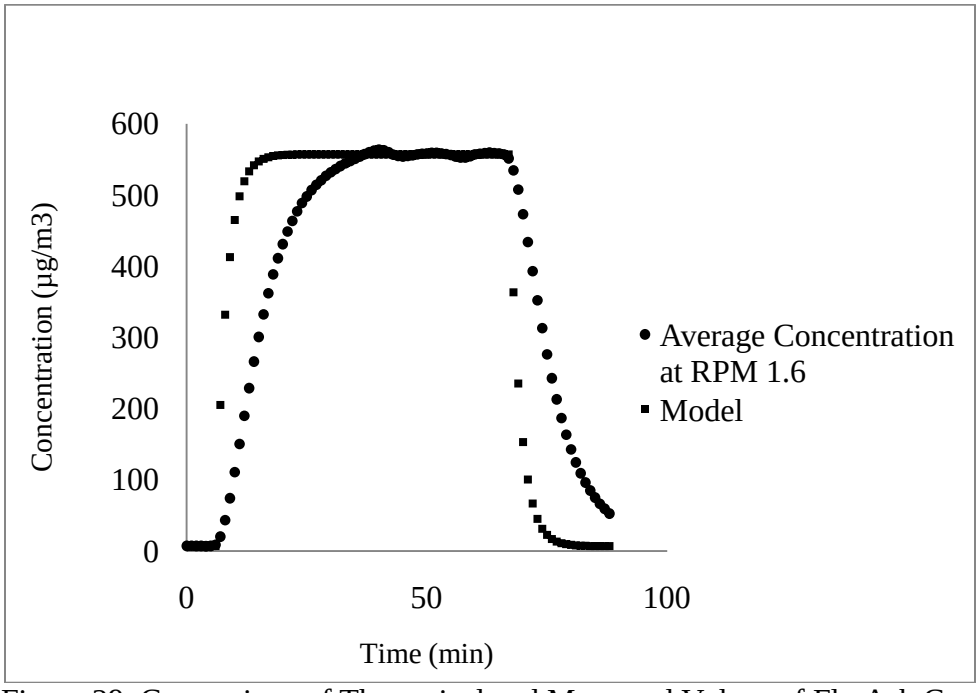

Figure 29. Comparison of Theoretical and Measured Values of Fly Ash Concentration at a Rate of Generation of RPM 1.6.

The delay in buildup and decay of measured particle concentration is similar to our findings with carbon dioxide, but greater in magnitude. This increased lag time is due to differences in instrument performance. The direct reading instrument measuring particle concentration (TEOM) displays a moving average that is determined over a period of 10 minutes and is updated every 2 seconds, while the instrument for carbon dioxide provides near instantaneous readings.

The maximum concentrations values measured and those predicted by the model agree, and it is believed the actual buildup and decay profiles for gases and particulates are similarly close to the model, but the limits of the instruments used in the study make this not possible to demonstrate.

Total, inhalable and respirable dust concentrations were also determined at different RPM settings of the dust generator and correlated with the concentrations obtained with the TEOM. Total and inhalable dust concentrations were approximately 1.2 times higher than the concentrations measured by the TEOM. The coefficient of correlation for both regression lines were 0.992 and 0.997. These results are in agreement with results published elsewhere (Salter et al., 1999), (Soutar et al., 1999). Theoretically the vertical elutriator does not allow particles greater than 8 μm to enter the chamber. As a result, the inhalable button sampler and the 37 mm open face cassettes collected particles with similar size ranges. The inhalable fraction concentrations were found to be 99% of the total dust concentrations. The high correlation between the inhalable fraction and the total dust concentrations is due to the vertical elutriator. Respirable dust concentrations were 0.79 times the concentrations of the TEOM. Respirable dust concentrations also were found for account 67% of the total dust

concentrations by gravimetric analysis.

Particle Size Distributions

Mass median diameters and geometric standard deviations were obtained by plotting the particle size distribution data on a log-probability chart. Mass median diameters ranged from 1.15 µm to 1.46 µm. Geometric standard deviations ranged from 2.08 to 2.35. Particle size distributions were found not to be statistically different regardless of the RPM settings of the dust generator. These results were expected because the same batch of fly ash was used for all dust generations and flowrates were similar.

In conclusion, the whole-body human exposure chamber at the USF Sunshine ERC Breath Laboratory will be a useful tool for inhalation challenge studies.

Limitations and Recommendations

The data obtained during the course of this research applies only to this exposure chamber and cannot be applied to any another inhalation challenge system. Dust concentrations and particle size of the test materials are only representative of the fly ash used, the air and nitrogen flowrates, and the rates of generation used during this study. This study did not evaluate the health effects of fly ash or carbon dioxide and no actual inhalation challenge research was conducted while characterizing and evaluating the performance this chamber.

For use of the chamber beyond the parameters of this study, further tests should be performed. For example utilization of a different type of dust, the presence of one or

more subjects in the chamber or the use of an ergometer will obviously be associated with changes in particle size distribution and particle concentration patterns in the chamber.

References

Aizemberg, V., Grinshpun, S., Willeke, K., Smith, J., Baron, P. (2000). Performance Characteristics of the Button Personal Inhalable Aerosol Sampler. American Industrial Hygiene Association Journal, 61(3), 398-404.

American Conference of Governmental Industrial Hygienists. (2009). Threshold Limit Values for Chemical Substances and Biological Exposure Indices. Cinncinnati Ohio: Author.

American Conference of Governmental Industrial Hygienists. (2010). Industrial Ventilation. A Manual of Recommended Practices. (27th Ed.) Cinncinnati Ohio: Author.

Bowes, S., Mason, E., Corn, M. (1993). Confined Space Ventilation: Tracer Gas Analyis of Mixing Characteristics. American Industrial Hygiene Association Journal, 54(11) , 639-646.

California Measurements, Inc. (2004). Instruction Manual- Air Partricle Analyzer Model PC-2 and PC-2H QCM Cascade Impactor. Sierra Madre, CA: Author.

Chen, C., Huang, S. H. (1998). The Effects of Particle Charge of a Filtering Facepiece. American Industrial Hygiene Association Journal , 59(4), 227-233.

Curtis, L., Rea, W., Smith-Willis, P., Fenyves, E., Pan, Y. (2006). Adverse Health Effects of Outdoor Air Pollutants. Environment International, 32, 815-830.

Esmen, N. (1978). Characteriation of Contaminant Concentrations in Enclosed Spaces. Environmental Science and Technology, 12(3), 337-339.

Fairchild, C., Wheat, L. (1984). Calibration and Evaluation of a Real-Time Cascade Impactor. American Industrial Hygiene Association Journal, 45(4), 205-211.

Feigley, C. E., Bennett, J. E., Lee, E., & Khan, J. (2002). Improving the Use of Mixing Factors for Dilution Ventilation Design. Applied Occupational and Environmental Hygiene, 17(5), 333-343.

Green, D., Kulle, T. (1986). Generation and Measurement of Formaldehyde in Exposure Chambers. Journal of Occupational and Environmental Hygiene, 47(8), 505-508.

Grenier, M., Hardcastle, S., Kunchur, G., Butler, K. (1992). The Use of Tracer Gases to Determine Dust Dispersion Patterns and Ventilation Parameters in a Mineral Processing Plant. American Industrial Hygiene Association Journal, 53 (6), 387-394.

Görner, P., Simon, X., Wrobel, R., Kauffer, E., Witchger, O. (2010). Laboratory Study of Selected Personal Inhalable Aerosol Samplers. Annals of Occupational Hygiene, 54 (2), 195-187.

Hammad, Y., Rando, R.H., Abdel-Kader, H. M.(1985). Considerations in the Design and Use of Human Inhalation Challenge Delivery Systems. Folia Allergologica et Immunologica Clinica, 32, 37-44.

Hammad, Y., Weill, H. (1980). Evaluation of Performance of a Beta Adsorption Dust Monitor. American Industrial Hygiene Association Journal , 41, 501 -507.

Hinds, W. C. (1999). Aerosol Technology. Properties, Behavior and Measurement of Airbone Particles, (2nd ed.). New York: John Wiley & Sons, Inc.

Horton, K., Ball, M., Mitchell, J. (1992). The Calibration of a California Measurementes PC-2 Quartz Crystal Cascade Impactor (QCM). Journal of Aerosol Science, 23(5), 505-524.

Ishizu, Y. (1980). General Equation of the Estimation of Indoor Pollution. Environmnetal Science and Technology ,14 (10), 1254-1257.

Jaylock, M. (1998). Assessment of Inhalation Exposure Potential from Vapors in the Workplace. American Industrial Hygiene Association Journal , 49 (8), 380-385.

Jönsson, B, Welinder, H, Skarping, G. (1994) Generation of Hexahydrophthalic Anhydride Atmospheres in a Controlled Human-Use Test Chamber. American Industrial Hygiene Association Journal, 55 (4), 330-338.

Leong, B. (1981). Inhalation Toxicology and Technology. Michigan: Ann Arnor Science Publishers, Inc.

Lidén C., Lundgren, L., Skare, G., Lidén, G., Tornlings, G., Krantz, S. (1998). A New Whole-Body Exposure Chamber for Human Skin and Lung Challenge Experiments – The Generation of Wheat Flour Aerosols. Annals of Occupational Hygiene, 42 (8), 541-547.

Linnainmaa, M., Laitinen, J., Leskinen, A., Sippula, O., Kalliolosli, P. (2008). Laboratory and Field Testing of Sampling Methods for Inhalable and Respirable Dust. Journal of Occupational and Environmental Hygiene, 5 (1), 28-35.

Lippmann, M., Albert, R. (1967). A Compact Electric-Motor Driven Spinning Disc Aerosol Generator. American Industrial Hygiene Association Journal, 28(6), 501-506.

Lundgren, L., Skare, L., Lidén, C., Tornling, G. (2006). Large Organic Aerosols in a Dynamic and Continous Whole- Body Exposure Chamber Tested on Human and on a Heated Mannequin. Annals of Occupational Hygiene, 50(7), 705-715.

Lund, K., Ekstrand, J., Boe, J., Søstrand, P., Kongerud, J. (1997). Exposure to Hydrogen Fluoride: An Experimental Study in Humans of Concentrations of Fluoride in Plasma, Symptoms, and Lung Function. Occupational and Environmental Medicine, 54, 32-37.

McClellan, R. O., Henderson, R. F. (1995). Concepts in Inhalation Toxicology, (2nd ed.). Washington, DC.: Taylor & Francis.

National Institute for Occupational Safety and Health. (1992). Analyzing Workplace Exposures Using Direct Reading Instruments and Video Exposure Monitoring Techniques (DHHS/NIOSH Publication No. 92-104). Washington, DC: Author.

National Institute for Occupational Safety and Health. (1994). Manual of Analythical Methods, Particulates Not Otherwise Regulated, Total, Method No. 0500. Washington, DC: Author.

National Institute for Occupational Safety and Health. (1998). Manual of Analythical Methods, Particulates Not Otherwise Regulated, Respirable, Method No. 0600. Washington, DC: Author.

O'Shaughenessy, P. T., Achutan, C., O'Neill, M., Thorne, P. (2003). A Small Whole-Body Exposure Chamber for Laboratory Use. Inhalation Toxicology, 15(3), 251-263.

O'Shaughenessy, P. T., Mehaffy, J., Watt, J., Sigurdarson, S., Kline, J. (2004). Characterization of a Hooded Human Exposure Apparatus for Inhalation of Gases and Aerosols. Journal of Occupational and Environmental Hygiene, 1(3), 161-166.

Page, S., Tuchman, D., Vinson, R. (2007). Thermally Induced Filter Bias in TEOM Mass Measurement. Journal Environmental Monitoring, 9, 760-767.

Popendorf, W. (2006). Industrial Hyiene Control of Airbone Chemical Hazards. Boca Raton, FL: CRC Press.

Reist, P. C., Taylor, L. (2000). Development and Operation of an Improved Turntable Dust Feeder. Powder Technology, 107(1), 36-42.

Rudell, B., Ledin, MC., Hammarström, U., Stjernberg, N., Lundäck, B., Sandström, T. (1996). Effects on Symptoms and Lung Function in Humans Experimentally Exposed to Diesel Exhaust. Occupational and Environmental Medicine, 53, 658-662.

Rupprecht & Patashnick Co., Inc. (2004). Service Manual TEOM Series 1400a Ambient Particulate (PM-10) Monitor (AB Serial Numbers). Albany, NY: Author.

Salem, H., Katz, S. A. (2006). Inhalation Toxicolgy, (2nd ed.). Boca Raton, FL: CRC Press.

Sällsten, G., Gustafson, P., Johansson, L., Johannesson, S., Molnár, P., Strandberg, B., Tullin, C., Barregard, L. (2006). Experimental Wood Smoke Exposure in Humans. Inhalation Toxicology, 18, 855-864.

Sandström, T., Stjernberg, N., Andersson, MC. Kolmodin-Hedman, B., Lundgren, R., Åmgström, T. (1989). Is the Short Term Limit Value for Sulphur Dioxide Exposure Safe? Effects of Controlled Chamber Exposure Investigated with Bronchalveolar Lavage. Brittish Journal of Industrial Medicine, 46, 200-203.

Salter, L., Parsons, B. (1999). Field Trials of the TEOM and Partisol for PM10 Monitoring in the St. Austell China Clay Aream Cornwall, UK. Atmospheric Environment, 33, 2111-2114.

Smith, J., Bartley, D., Watkins, D. (1999). Development of a Large Particle Aerosol Distribution System for Testing Manikin-Mounted Samplers. Aerosol Science and Technology, 30, 454-466.

Schiffman, S., Studwell, C., Landerman, L., Berman, K., Sundy, J. (2005) Symptomatic Effects of Exposure to Diluted Air Sampled from a Swine Confinement Atmosphere on Healthy Human Subjects. Environmental Health Perspectives, 113(5), 567-576.

Soutar, A., Watt, M., Cherrie, J., Seaton, A. (1999). Comparison between a Personal PM10 Sampling Head and the Tapered Element Oscillating Microbalance (TEOM) System. Atmospheric Environment, 33, 4373-4377.

Suarez, J., Warmath, S., Koetz, K., Hood, A., Thompson, M., Kendal-Reed, M., Walker, D., Walker, J. (2005). Single-Pass Environmental Chamber for Quantifying Human Responses to Airborne Chemicals. Inhalation Toxicology, 17, 169-175.

Sundblad, B-M., Larsson, B-M., Acevedo, F., Ernstgård, L, Johanson, G., Larsson, K., Palmberg, L. (2004). Acute Respiratory Effects of Exposure to Ammonia on Healthy Persons. Scandinavian Journal of Work, Environment & Health, 30(4), 313-321.

Taylor, L., Reist, P., Boehlecke, B., Jacobs, R. (2000). Characterization of an Aerosol Chamber for Human Exposures to Endotoxin. Applied Occupational and Environmental Hygiene, 15(3),303-312.

Tuomainen, A., Stark, H., Seuri, M., Hirvonen, M-R., Linnainmaa, M., Sieppi. A. (2006). Experimental PVC Material Challenge in Subjects with Occupational PVC Exposure. Environmental Health Perspectives, 114(9), 1409-1413.

Tzou, T. (1999). Aerodynamic Particle Size of Metered-Dose Inhalers Determined by the Quartz Crystal Microbalance and the Andersen Cascade Impactor. International Journal of Pharmaceutics, 186, 71-79.

Vincent, J. (2007). Aerosol Sampling. Sscience, Standards, Instrumentation and Applications. England: John Wiley & Sons Ltd.

Walton, W. H. (1954). Theory of Size cCassification of Airborne Dust Clouds by Elutriation. Brittish Journal of Applied Physics, 5, S29-S37.

Wanjura, J., Shaw, B., Parnell, C., Lacey, R., Capareda, S. (2008). Comparisons of Continuous Monitor (TEOM) and Gravimetric Sampler Particulate Matter Concentrations. American Society of Agricultural and Biological Engineers, 51(1), 251-257.

Willeke, K. (1980). Generation of Aerosols and Facilities for Exposure Experiments. Michigan: Ann Arbor Science Publishers, Inc.

Wong, B. A. (2007). Inhalation Exposure Systems: Design, Methods and Operation. Toxicologic Pathology, 35(1) , 3-14.

Wright, B. M. (1950). A New Dust-Feed Mechanism. Journal of Scientific Instrument, 27, 12-15.

Zhou, Y.,Cheng, Y-S. (2010). Evaluation of IOM Personal Sampler at Different Flow Rates. Journal of Occupational and Environmental Hygiene, 7(2), 88-93.

Appendices

Appendix A: Calibration of Orifice Meters

Orifice meter calibrations were performed using a Micro-Pitot tube. Flowrate was determined using Equation 12.

Table VIII. Calibration of Orifice Meter OM-1A Using a Micro-Pitot Tube.

3 in.wg			4 in.wg			5 in.wg		
Pitot Tube Reading in. wg.	Flow L/min	OM Reading in.wg.	Pitot Tube Reading in. wg.	Flow L/min	OM Reading in.wg.	Pitot Tube Reading in. wg.	Flow L/min	OM Reading in.wg.
0.27	652	0.9	0.26	640	0.9	0.24	615	0.9
0.34	732	1.2	0.29	676	1.1	0.28	664	1.1
0.39	784	1.5	0.37	764	1.4	0.32	710	1.3
0.45	842	1.7	0.45	842	1.6	0.4	794	1.6
0.48	870	1.8	0.48	870	1.8	0.44	833	1.8
			0.49	879	2	0.53	914	2
			0.54	923	2.2	0.56	940	2.3
			0.59	964	2.3	0.62	989	2.5
			0.63	997	2.4	0.67	1028	2.6

Table IX. Calibration of Orifice Meter OM-1B Using a Micro-Pitot.

3 in.wg			4 in.wg			5 in.wg		
Pitot Tube Reading in. wg.	Flow L/min	OM Reading in.wg.	Pitot Tube Reading in. wg.	Flow L/min	OM Reading in.wg.	Pitot Tube Reading in. wg.	Flow L/min	OM Reading in.wg.
0.23	602	0.9	0.19	547	0.8	0.26	640	0.9
0.31	699	1.4	0.25	628	1.1	0.27	652	1.1
0.38	774	1.6	0.31	699	1.3	0.37	764	1.6
0.41	804	1.8	0.43	823	1.7	0.38	774	1.8
0.47	861	2	0.5	888	2	0.48	870	2.1
			0.53	914	2.3	0.53	914	2.4
						0.58	956	2.6
						0.61	981	2.7
						0.64	1004	2.8
						0.71	1058	3

Appendix B: Carbon Dioxide Measurements

Measurements of carbon dioxide volume were obtained using a dry gas meter. Flow rate of the system was calculated using orifice meter's calibration equations.

Table X. Carbon Dioxide Flow Rates at Different Rates of Generation.

	Run 1	Run 2	Run 3
Total Volume (L)	47.6	85.7	110
Time (min)	10	10	10
Flow Rate (L/min)	4.76	8.57	11.0
Background Concentration (ppm)	444	532	484
Average System Flow Rate (L/min)	951	970	980

Appendix C: Calibration of Nitrogen Flowrate

Calibration of rotameter was made using a TSI mass flow meter (MFM), model 4146 (Shoreview, MN.).

Table XI. Calibration of Rotameter at Different Flowrates of Nitrogen.

Rotameter	MFM (L/min)
10	2.21
20	4.9
30	7.55
40	10.2
50	13
60	15.8
70	18.9
80	21.8
90	24.9

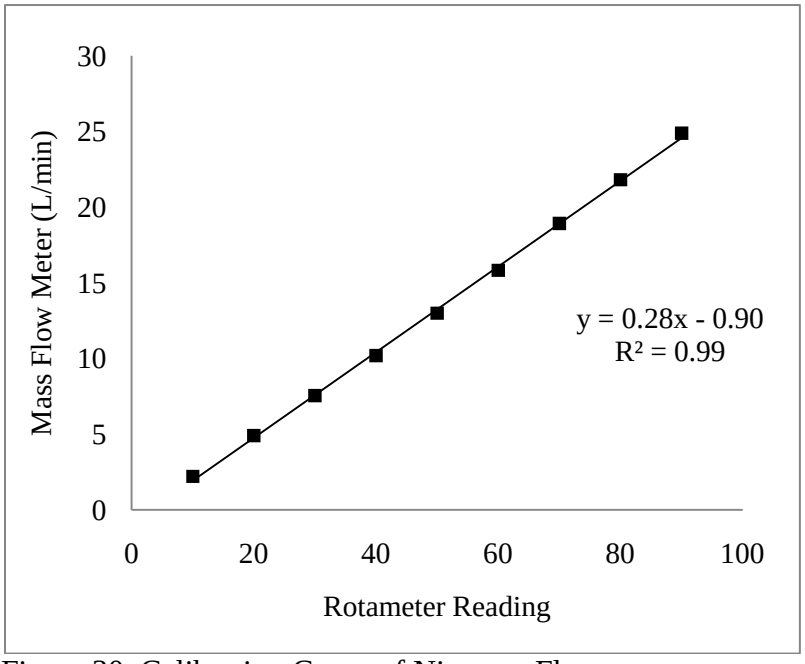

Figure 30. Calibration Curve of Nitrogen Flowrate.

Appendix D: Determination of the Cut-Off Particle Diameter of the Vertical Elutriator

The determination of the velocity of nitrogen through the vertical elutriator was obtained using Equation 13, where the flowrate of nitrogen was determined using the regression equation of Figure 28. The area was determined using Equation 23.

$$\text{Area} = \pi * r^2 \qquad (23)$$

The diameter measured was 18.69 cm with a radius of 9.346 cm. The area of the circle was determined to be 274.27 cm^2. Using Equation 13, the velocity of the nitrogen in the vertical elutriator was 0.51 cm/sec.

The calculation of the diameter of the fly ash particle passing the vertical elutriator was made using Equation 14 where the viscosity of the nitrogen is 0.000175 poise, the density of the fly ash is 2.65 g/cm^3 and acceleration due to gravity is 981 cm/sec^2 (Hinds, 1999).

$$d = \sqrt{\frac{(0.51 \text{ cm/sec})(18)(0.000175 \text{ gm/cm sec})}{(2.65 \text{ gm/cm}^3)(981 \text{ cm/sec}^2)}}$$

$$d = 0.000786 \text{ cm}$$

$$d = 7.86 \text{ µm}$$

The theoretical diameter of the fly ash particles passing the elutriator and entering to the system is about 8 µm or lower.

Appendix E: TEOM Dust Concentrations

Table XII. TEOM Dust Concentrations at RPM 0.2

Time (min)	First Run ($\mu g/m^3$)	Second Run ($\mu g/m^3$)	Third Run ($\mu g/m^3$)	Fourth Run ($\mu g/m^3$)	Fifth Run ($\mu g/m^3$)
1	3.4	8.6	8.7	9.2	9.7
2	3.6	7.9	7.5	9.2	9.3
3	3	8	5.7	9.3	9.8
4	3	7.3	5.5	9.1	10
5	3.2	8.1	3.6	9.4	10.1
6	3.1	7.5	3.1	9.4	9.5
7	6.7	9.6	5	10.8	10.6
8	19	17.3	13.6	20.2	18.2
9	36	30.1	27	32.5	29.3
10	52.1	43.8	39.9	45	40.5
11	66.7	55.9	54.1	55.4	50.3
12	78.1	66	66.4	63.8	59.2
13	86.1	73.6	75.2	70.6	67
14	92.1	80	82.4	76.3	73.5
15	96.2	84.1	87.7	81.2	77.4
16	99.4	86.7	91.4	84.5	81.9
17	101.7	89.3	94.9	86.3	85.7
18	104.3	90.9	97.5	88.4	88.2
19	105	91.7	99	90.2	92.2
20	106.3	93.3	99.9	92.2	96.6
21	105.6	94.3	101	93.5	100.3
22	104.7	95.8	102.4	95.7	103.5
23	105.1	96.8	103.4	95.7	106.5
24	105.5	98.3	104.5	96.9	108.2
25	106.1	99.7	105.1	97.8	110.1
26	106.2	100.8	105.1	99.8	111.5
27	105.1	102.3	104.8	101	111.3
28	103.4	103.7	104.9	100.8	111.9
29	102.6	104.5	105.2	101	112
30	102.5	105.8	106.7	100.1	112.2
31	102.4	106.2	107.1	101.2	112
32	102.4	106	108.7	102.3	113.1

Table XII. TEOM Dust Concentrations at RPM 0.2 (continued)

Time (min)	First Run ($\mu g/m^3$)	Second Run ($\mu g/m^3$)	Third Run ($\mu g/m^3$)	Fourth Run ($\mu g/m^3$)	Fifth Run ($\mu g/m^3$)
33	102.3	107.1	110.3	102.1	113.6
34	102.4	108.3	111.7	103.6	114.9
35	102.6	108	112.9	104.5	116.4
36	103.4	108	113.5	106.3	117.6
37	103.8	109.1	114.9	107.5	119.6
38	104.1	110.3	115.6	108.8	120.6
39	104.6	111.4	115.3	109.5	120.7
40	105.5	112.2	116.1	110.3	119.6
41	105.5	113.2	117.2	110.2	120.4
42	106.5	113.5	118.9	110.8	120.2
43	107	113.2	119	111.5	118.8
44	107.6	112.8	120.1	111.3	118.1
45	107.5	111.6	119.8	110.7	118.2
46	107.5	111.2	119.7	110.7	119.2
47	107.6	110.3	118.9	110.7	120.4
48	108	109.2	117.8	110.4	120.8
49	108.4	108.7	117.5	111.4	121.7
50	107.4	108.7	116.9	110.7	121.9
51	108.2	109.6	115.6	110.7	123.7
52	108.3	111.3	115.4	111.8	125
53	108.1	113.6	114	113.4	126.3
54	108.1	115.4	112.1	114.2	126.5
55	108.3	116.2	111.4	114.4	127.2
56	107.8	118	109.7	114.9	126.9
57	107.5	118.6	109.2	114.9	126.1
58	106.6	120	109.6	116	125.7
59	107.4	120.2	110.1	117	124.6
60	108.2	121	111.3	115.8	122.8
61	108.1	120.7	112.2	114.9	120.2
62	108.7	119.9	112	113.6	118.8
63	108.8	117.3	111.6	112.3	118.3
64	109.8	116.6	111.3	111.7	117.6

Table XII. TEOM Dust Concentrations at RPM 0.2 (continued)

Time (min)	First Run ($\mu g/m^3$)	Second Run ($\mu g/m^3$)	Third Run ($\mu g/m^3$)	Fourth Run ($\mu g/m^3$)	Fifth Run ($\mu g/m^3$)
65	110.2	114.4	111.9	110.5	115.2
66	109	113.1	112.2	110.4	110.8
67	108.4	112	112.1	110.7	104
68	107.5	109.4	110.4	110.4	96.5
69	106	105.8	107.1	108.4	87.4
70	102.9	99.9	102.5	104.2	79
71	97.5	93.2	94.8	97.4	70
72	91.4	84.1	86.7	89.6	62.4
73	84	75.8	79	82.6	55.9
74	76.2	67.2	70.6	74.7	49.3
75	68.4	58.9	63.7	65.6	44
76	59.9	51.9	56.3	58.9	38.5
77	51.1	44.9	49.4	53	33.8
78	44.3	39.7	44.4	46.6	30.5
79	38.6	36.3	39.2	40.8	27.4
80	33.8	33.2	33.5	36.7	24.5
81	28.8	28.8	29.5	32.7	21.7
82	25.3	25.3	25.8	30	19.9
83	23.5	22	22.9	26.9	18.7
84	21.8	19.8	20.7	23.8	17.5
85	19.4	17.8	18.8	21.3	16.4
86	16.4	16.5	17.7	18.8	15.1
87	14.6	15.2	16.2	17.1	14

Table XIII. TEOM Dust Concentrations at RPM 0.4

Time (min)	First Run ($\mu g/m^3$)	Second Run ($\mu g/m^3$)	Third Run ($\mu g/m^3$)	Fourth Run ($\mu g/m^3$)	Fifth Run ($\mu g/m^3$)
1	1.6	2.4	-0.6	10.5	1.8
2	2.9	2.9	-0.6	10.2	2.2
3	2.6	2.4	0	10.3	2.8
4	2.4	2.3	-0.6	11.9	2.4
5	2.5	2.2	-0.4	12.3	2.7
6	2.2	1.1	-0.9	12.3	3.1
7	3.3	3.3	-0.7	13.4	5.1
8	14.2	8	3.6	16.1	13
9	30.3	15.2	13.5	21.7	24.9
10	48.2	23.8	24.5	28.2	39.1
11	64.3	33.7	37.1	38	52.2
12	78.9	45.2	49.7	47.5	65.2
13	94.1	59	62.8	58.5	77.3
14	106.6	71.2	73.1	67.9	87.9
15	117.4	80.2	84.8	75.5	96.8
16	127.6	91.8	94.7	84.4	106.6
17	137.5	101.5	103.1	92.3	114.7
18	146	111.4	110	100	121.2
19	154.5	119.5	117	106.4	127.6
20	161.4	127.1	123.2	112.7	133.3
21	167.2	133.3	129.2	119.6	138.7
22	172.2	138.1	134.3	125.5	144.1
23	177.7	145	138.3	130.3	148.5
24	182.5	150.5	143.1	134.2	152
25	185.6	153.7	145.7	136.8	155.2
26	189.9	156.2	149.3	140.4	158.7
27	192.4	158.5	152	144.4	161.3
28	195.7	160.8	153.7	146.8	163.3
29	197.7	162.9	156.9	148.6	166.9
30	200.9	163.5	158.9	150.4	171.1
31	202.8	165.4	161.3	152	173
32	204.2	165.9	162.1	154.7	175.6

Table XIII. TEOM Dust Concentrations at RPM 0.4 (continued)

Time (min)	First Run ($\mu g/m^3$)	Second Run ($\mu g/m^3$)	Third Run ($\mu g/m^3$)	Fourth Run ($\mu g/m^3$)	Fifth Run ($\mu g/m^3$)
33	205.6	166.5	164.1	156.7	176.6
34	206.2	167.4	165.4	158.3	178.5
35	206.8	167.5	165.5	159.9	180.9
36	207.4	168.3	165.8	161.1	181.7
37	209.9	168.4	166.7	161.7	182.2
38	210.3	168.1	167.3	163	182.6
39	210.9	168.7	168	162.8	183.1
40	211.9	168.3	169	163.2	184.1
41	213	169.3	169.8	163.5	184.5
42	213.2	169.5	171	163.1	185.3
43	214.3	169.5	172.5	164.4	186.1
44	214.5	169	173	165.5	185.6
45	215.3	168.7	173.2	165.1	185.4
46	215.5	168.6	174.7	165.7	184.9
47	215.1	167.4	174.6	165.9	185.7
48	214.1	167.3	174.4	166.6	186.3
49	214.2	168.8	174.5	168.1	186.5
50	215.2	168.8	176.2	168.5	186.3
51	214.3	169.9	176.2	168.8	187.5
52	213.4	168.9	176.6	169.1	188.7
53	213.9	169.5	175.9	169.8	191
54	213.9	169.6	177.3	170.3	191.4
55	213.9	168.7	176.1	170.3	192
56	213.5	169.4	175.3	171.1	192.2
57	213.6	168.4	175.2	170.6	193.1
58	213.9	168.5	174.9	170.1	193.2
59	215	167.5	174.2	170.5	192.6
60	215.6	168.3	175	170.4	191.6
61	215.1	169.1	175.2	169.9	192
62	214.8	170.6	176.1	171	192.1
63	213.9	170.3	176.4	171.9	192.3
64	213.8	169.9	176	172.5	192.5

Table XIII. TEOM Dust Concentrations at RPM 0.4 (continued)

Time (min)	First Run ($\mu g/m^3$)	Second Run ($\mu g/m^3$)	Third Run ($\mu g/m^3$)	Fourth Run ($\mu g/m^3$)	Fifth Run ($\mu g/m^3$)
65	213	169.8	175.3	172.6	191.1
66	211.9	168.9	175.7	172.8	189.8
67	212.6	167.2	176.1	171.9	190.6
68	211.5	165.7	175.1	170.7	188.8
69	206.1	161.8	169.4	165.5	183
70	196.3	153.3	160.8	156.4	174.3
71	182.5	142.6	149.1	144.9	162.4
72	167.2	130.6	136.9	131.9	147.9
73	150.9	115.8	123.4	117.9	132
74	134.4	103.1	110.2	104.2	117
75	118	91.8	97	92.9	101.9
76	103.5	81.2	84.5	83.2	90.2
77	90.4	71.5	74.3	72.6	76.6
78	78.9	60.4	64.3	62.8	65.9
79	68	52	55.6	53.3	57.5
80	59	44.4	47.9	45.7	48.7
81	50.5	38.3	40.4	39.6	41.5
82	42.9	34.2	34.1	34.4	36
83	35.7	28.9	30.1	28.9	30.5
84	31	24.5	26.2	25	26.3
85	27.7	21.3	22.9	22.1	22.5
86	23.7	17.7	20.3	20	19.9
87	20.7	14.9	16.8	17.4	17

Table XIV. TEOM Dust Concentrations at RPM 0.8

Time (min)	First Run ($\mu g/m^3$)	Second Run ($\mu g/m^3$)	Third Run ($\mu g/m^3$)	Fourth Run ($\mu g/m^3$)	Fifth Run ($\mu g/m^3$)
1	27.8	3.9	2.7	2.8	-0.8
2	25.2	3.9	2.6	3.3	-0.2
3	23.4	2.8	2.9	2.3	-0.4
4	21.8	2.4	3.8	2.8	0
5	20.3	3.9	3.8	3.7	-0.4
6	17.9	4.8	3.6	3.3	-0.4
7	16.3	5.9	6.2	5.6	4.8
8	18.3	9.8	21.5	13.8	27.1
9	26.1	19.2	47.2	26.5	58.4
10	41.7	37.8	80.1	40.6	89.9
11	64	63	115.1	56.1	118.5
12	93.2	93.8	151.5	73.3	145.1
13	126.2	128.8	187.1	91.7	168.8
14	159.2	165.6	218.2	111.9	189.9
15	191.6	202.6	246.9	132.6	209.4
16	221.2	237.2	273.1	153.2	227.2
17	248	268.2	294.8	172.5	244.5
18	272.1	298.6	313.3	192.2	260.6
19	293	325.3	330.8	210.7	274.6
20	312.8	348.1	345	228.8	288
21	329.2	369.1	357.4	246.3	300.2
22	344	386.9	367.6	263.3	312.3
23	356.3	402.5	375.4	279.5	323
24	368	415.8	382.7	293	332.9
25	377.4	429.1	390	307.1	341.7
26	384.3	441.5	398.3	318.6	350.7
27	390.9	451.3	405	327.8	358.4
28	396	461.6	409.8	335.5	365.2
29	400.3	469.5	413	342.4	371.4
30	404.3	476.8	413.3	348.4	376.8
31	408.8	482	413.6	353.6	381.3
32	410.4	485.5	413.3	358.4	386.2

Table XIV. TEOM Dust Concentrations at RPM 0.8 (continued)

Time (min)	First Run ($\mu g/m^3$)	Second Run ($\mu g/m^3$)	Third Run ($\mu g/m^3$)	Fourth Run ($\mu g/m^3$)	Fifth Run ($\mu g/m^3$)
33	412.4	485.6	413.9	362.9	390.9
34	411.3	487	415.4	367.6	395
35	412.9	485.6	416.2	371.2	398.8
36	414.5	487.9	416.6	373.6	401.9
37	413.5	489.2	417.4	376.1	403.5
38	414	490.8	417.5	379.9	405.8
39	414.2	492.1	417.3	383.3	406.5
40	416.2	488.1	418	386.9	408.2
41	418.1	487.2	419.3	388.9	408.9
42	418	495.9	418.8	388.1	410.6
43	417.3	505.2	419.2	387.4	412.8
44	415.8	507.2	418.5	388.6	415.2
45	412.7	508.7	419.2	387.6	416.7
46	411.8	509.8	421.8	389.3	416.7
47	404.2	508.9	424.4	391.6	417.4
48	399.9	507.3	424.4	394.3	418.7
49	396.1	505.8	423	397.3	420.2
50	394.8	504.6	420.7	398.8	420.8
51	394.5	503.3	420.6	399.9	419.8
52	394.8	501	420.3	399.8	420.1
53	396.9	500.1	420.8	400.5	421.9
54	398.8	498.7	421.5	401.4	421.9
55	399.4	498.7	423.7	403.2	421.2
56	401.3	501.7	425.8	403.8	421.2
57	403.8	509.2	428.2	403.2	421.1
58	405.2	515.2	431.5	404.6	421.6
59	407.5	521.7	435	404.4	421.1
60	408.7	520.5	438.4	405.8	421.7
61	408.8	511.9	443	405.7	420.5
62	407.8	502.6	444.8	406.3	420.7
63	407.2	495.8	446.9	406.7	420.8
64	406.3	492	448.4	406.9	421.9

Table XIV. TEOM Dust Concentrations at RPM 0.8 (continued)

Time (min)	First Run ($\mu g/m^3$)	Second Run ($\mu g/m^3$)	Third Run ($\mu g/m^3$)	Fourth Run ($\mu g/m^3$)	Fifth Run ($\mu g/m^3$)
65	405.7	490.8	449.8	407.5	423.4
66	405.9	489.3	450.7	407.3	424.4
67	404.7	490.3	446.6	407.7	425.2
68	399.7	485.3	432.9	404.6	420.8
69	387.5	468.3	409.8	393.3	407.7
70	366.5	441.7	379.4	373.5	385.6
71	338.7	406.7	345.1	346.7	356.5
72	308.2	368.2	309.6	315.3	324.8
73	276.3	328	274.3	282.3	292
74	244.9	288.6	240.3	249.9	260.8
75	214.8	252	209.3	219	230.3
76	187	217.9	181.5	190.6	202.2
77	161.6	187.6	156.1	164.8	176.4
78	139.6	161.4	134.1	141.5	153.5
79	120.2	138	114.8	121.5	133.4
80	102.9	117.9	98.3	103.6	114.9
81	88.5	100.9	84.4	89	99.4
82	76.3	86.7	72.8	75	84.4
83	65.7	74.1	62.9	64	72.7
84	56.4	63.2	54.6	55.3	62.8
85	49	54	47	46.8	54.1
86	41.9	46.3	41.3	40.4	46.8
87	36.1	40.4	36.4	35.4	41
88	31.2	34.7	32.2	30.8	35.7
89	28.3	29.9	27.8	26.5	31.2

Table XV. TEOM Dust Concentrations at RPM 1.6

Time (min)	First Run ($\mu g/m^3$)	Second Run ($\mu g/m^3$)	Third Run ($\mu g/m^3$)	Fourth Run ($\mu g/m^3$)	Fifth Run ($\mu g/m^3$)
1	2.5	5	11.5	5.5	12
2	2.7	5.3	11	5.2	13.2
3	2.9	5.2	10.4	4.9	13.1
4	3.6	5.7	11.5	4.6	11.4
5	2.9	4.6	10.9	4.2	11.4
6	2.8	6.2	10.6	4.3	12.5
7	2.9	7.1	13	8.2	12.8
8	13.8	13.4	25.5	27.1	22.3
9	35.6	31.3	50.3	56.6	43.8
10	64.9	56.9	81.8	92.4	75.8
11	97.9	91.4	120.2	130.9	114.3
12	135.7	129.4	158.6	171.1	157.1
13	174.3	166.8	196.8	210.8	201.8
14	212.4	205.7	236	248.3	242
15	250	244.4	272.4	283.3	280.7
16	286.4	280.7	307.3	316.1	313.7
17	320.9	312.6	337.9	346.3	345.3
18	353.5	340.9	366.1	376	374.1
19	382.4	366.3	392.4	402.1	399.6
20	406.3	388.6	415.3	425.7	421.2
21	428.9	408.1	435.5	444.2	439.2
22	449	426.3	453.4	461.2	454.3
23	467.2	442.4	467.5	475	466.9
24	483.2	457.5	479.2	488.2	478.1
25	496.8	470.4	489.7	500	486.8
26	507.5	480.5	498.8	509.3	494.7
27	518.6	490.4	507.7	518	500.7
28	526.8	498.1	515	525.8	506.2
29	534.3	503.6	521.6	532.1	512.1
30	542.1	508.8	529.7	537.5	517.2
31	548.7	512.1	537	542.2	519.9
32	552.4	516	543.1	546.9	524.5

Table XV. TEOM Dust Concentrations at RPM 1.6 (continued)

Time (min)	First Run ($\mu g/m^3$)	Second Run ($\mu g/m^3$)	Third Run ($\mu g/m^3$)	Fourth Run ($\mu g/m^3$)	Fifth Run ($\mu g/m^3$)
33	556.6	520.7	548	551	527.6
34	557.9	525.6	553.8	555.2	531.3
35	559.5	528.2	558.5	559.3	533.5
36	561.8	530.6	561.7	566	535.1
37	562.8	531	563.5	574.8	538.8
38	564	530.6	571.3	581.7	539.8
39	565.6	529.8	581	584.9	540.7
40	567.3	529	589.1	585.5	541
41	569.6	526.8	593.2	584.7	544.7
42	571	525.3	592.5	579.9	546.1
43	572.3	523.6	587.2	572.3	546.6
44	573.8	521	582.3	564.4	543
45	574.9	520.2	580.9	559.2	539.9
46	575.4	519.5	583.9	557.7	534.7
47	577.7	520.4	586.9	558.5	531.1
48	579.2	522.3	589.4	559.4	529.7
49	580.2	524	590.6	560.7	529.9
50	580.2	527.4	587.5	564.4	531.2
51	578.5	533.8	579.3	567	533.8
52	578.2	542.4	569.3	569.3	537.9
53	577.7	547	559.2	569.8	543.6
54	577.3	548.4	552.7	566.9	547.5
55	577.3	548.5	549.1	563.2	549.5
56	577.8	545.9	548.8	560.4	548.9
57	576.6	538.5	550.2	558.4	545.9
58	577.4	531.6	554.1	557.3	543
59	578.7	527.4	558	558.9	541.3
60	581.3	524.9	559.8	566.8	540.4
61	585.2	523.9	557.7	578.2	540.6
62	584.2	521.4	554.7	587.5	543.2
63	583.5	520.5	552.8	592.6	545.6
64	582.8	519.4	550.6	595.3	550

Table XV. TEOM Dust Concentrations at RPM 1.6 (continued)

Time (min)	First Run ($\mu g/m^3$)	Second Run ($\mu g/m^3$)	Third Run ($\mu g/m^3$)	Fourth Run ($\mu g/m^3$)	Fifth Run ($\mu g/m^3$)
65	582.6	518.2	546.8	594.1	553.2
66	580.9	518.4	545	590.8	557
67	579.8	521.3	543.5	583.7	558
68	572.9	524.6	537.7	570	552.5
69	554.6	514.1	521.1	547.3	536.5
70	526.4	492.3	494.7	515.8	509.1
71	490.4	461.7	462	477	475.2
72	447.9	424.7	424.8	435.3	436.9
73	403	386.1	385.5	391.6	399.3
74	359.5	346.9	346.4	349.5	359.5
75	317.1	308.9	309	309.5	320.9
76	277.4	273	273.7	272.4	284.4
77	241.7	240	241.3	239.3	251.8
78	210.9	210.1	213.9	209.1	221.8
79	182.8	183.9	188.6	183.3	195.2
80	159.1	161.4	165.3	159.5	171.9
81	138.1	140.4	144.6	139	151.9
82	119.2	122.6	126.7	121.4	133.3
83	103.9	106.4	112.8	106.1	117.3
84	91.4	93.2	100	93.6	103.1
85	79.8	82	90.5	82	91.3
86	70.3	71.7	80.4	72.7	80.9
87	61.8	62.1	71.7	64.4	71.7
88	54.3	55	66.3	57.4	64.2
89	47.8	48.2	59.8	50.4	57.3
90	41.6	43.6	54.6	45.1	52.2
91	38.3	38.1	49.7	39.8	46.7
92	34.5	33.8	45.9	36.7	42.7
93	31.7	30.1	43.3	33.7	39.7
94	28.1	28.6	40.3	30.4	37.4
95	25.4	25.7	37.1	27.5	35.4

Appendix F: Air Pump Calibration

Air pumps where pre and post calibrated for each run with BIOS Defender 510-M.

Table XVI. Pre and Post Calibration of Pumps for Generation at RPM 0.2

Pump Model	SKC 35287		SKC 35304		MSA A3-45688	
	Pre (L/min)	Post (L/min)	Pre (L/min)	Post (L/min)	Pre (L/min)	Post (L/min)
1	2.500	2.472	2.506	2.490	2.521	2.499
2	2.506	2.477	2.513	2.507	2.522	2.520
3	2.523	2.474	2.504	2.490	2.521	2.501
4	2.518	2.493	2.525	2.485	2.536	2.501
5	2.527	2.486	2.485	2.480	2.535	2.492
6	2.505	2.491	2.507	2.476	2.526	2.498
7	2.534	2.493	2.514	2.502	2.539	2.491
8	2.513	2.479	2.520	2.495	2.520	2.491
9	2.495	2.479	2.492	2.494	2.535	2.491
10	2.522	2.479	2.527	2.501	2.532	2.493
Average	2.514	2.482	2.509	2.492	2.529	2.498
SD	0.01269	0.00772	0.01363	0.00987	0.00730	0.00896
CV	0.505%	0.311%	0.543%	0.396%	0.289%	0.359%
Average Flow	2.498		2.501		2.513	

Table XVI. Pre and Post Calibration of Pumps for Generation at RPM 0.2 (continued)

Pump Model	MSA A3-45690		MSA A3-45688	
	Pre (L/min)	Post (L/min)	Pre (L/min)	Post (L/min)
1	2.500	2.489	2.4833	2.4992
2	2.506	2.491	2.4675	2.5032
3	2.497	2.490	2.4675	2.4905
4	2.513	2.488	2.4869	2.4874
5	2.504	2.491	2.4905	2.4981
6	2.499	2.490	2.4874	2.4864
7	2.494	2.488	2.4776	2.4909
8	2.513	2.488	2.493	2.4951
9	2.503	2.488	2.4854	2.5007
10	2.508	2.488	2.4823	2.4879
Average	2.504	2.489	2.482	2.494
SD	0.00633	0.00118	0.00882	0.00610
CV	0.253%	0.047%	0.355%	0.245%
Average Flow	2.496		2.488	

Air pumps where pre and post calibrated for each run with BIOS Defender 510-M.

Table XVII. Pre and Post Calibration of Pumps for Generation at RPM 0.4

Pump Model	MSA A3-45690		MSA A3-45688		MSA A3-45691	
	Pre (L/min)	Post (L/min)	Pre (L/min)	Post (L/min)	Pre (L/min)	Post (L/min)
1	2.498	2.488	2.524	2.486	2.497	2.511
2	2.507	2.491	2.521	2.477	2.495	2.521
3	2.495	2.494	2.510	2.483	2.505	2.510
4	2.506	2.493	2.513	2.471	2.503	2.514
5	2.501	2.491	2.510	2.472	2.508	2.513
6	2.498	2.491	2.521	2.468	2.495	2.501
7	2.497	2.492	2.517	2.475	2.492	2.502
8	2.498	2.493	2.517	2.473	2.504	2.523
9	2.494	2.492	2.507	2.478	2.510	2.526
10	2.498	2.489	2.508	2.468	2.497	2.529
Average	2.499	2.491	2.515	2.475	2.500	2.515
SD	0.00444	0.00179	0.00606	0.00605	0.00609	0.00951
CV	0.177%	0.072%	0.241%	0.245%	0.244%	0.378%
Average Flow	2.495		2.495		2.508	

Table XVII. Pre and Post Calibration of Pumps for Generation at RPM 0.4 (continued)

Pump Model	MSA A3-45687		MSA A3-45688	
	Pre (L/min)	Post (L/min)	Pre (L/min)	Post (L/min)
1	2.510	2.489	2.513	2.519
2	2.514	2.498	2.482	2.516
3	2.506	2.498	2.516	2.494
4	2.502	2.499	2.517	2.526
5	2.512	2.490	2.517	2.488
6	2.508	2.490	2.505	2.512
7	2.509	2.502	2.521	2.518
8	2.502	2.500	2.485	2.511
9	2.504	2.496	2.478	2.508
10	2.510	2.491	2.507	2.490
Average	2.508	2.495	2.504	2.508
SD	0.00417	0.00483	0.01631	0.01318
CV	0.166%	0.193%	0.651%	0.526%
Average Flow	2.501		2.506	

Air pumps where pre and post calibrated for each run with BIOS Defender 510-M.

Table XVIII. Pre and Post Calibration of Pumps for Generation at RPM 0.8

Pump Model	MSA A3-45691		MSA A3-45687		MSA A3-45690	
	Pre (L/min)	Post (L/min)	Pre (L/min)	Post (L/min)	Pre (L/min)	Post (L/min)
1	2.513	2.466	2.499	2.467	2.483	2.445
2	2.512	2.478	2.512	2.469	2.480	2.445
3	2.511	2.485	2.501	2.458	2.482	2.449
4	2.513	2.472	2.511	2.467	2.489	2.446
5	2.491	2.490	2.508	2.467	2.479	2.445
6	2.506	2.482	2.502	2.469	2.484	2.446
7	2.494	2.480	2.518	2.473	2.481	2.443
8	2.494	2.473	2.502	2.455	2.484	2.444
9	2.501	2.485	2.504	2.460	2.482	2.446
10	2.492	2.469	2.503	2.461	2.486	2.443
Average	2.503	2.478	2.506	2.465	2.483	2.445
SD	0.00919	0.00780	0.00600	0.00579	0.00301	0.00171
CV	0.367%	0.315%	0.240%	0.235%	0.121%	0.070%
Average Flow	2.490		2.485		2.464	

Table XVIII. Pre and Post Calibration of Pumps for Generation at RPM 0.8 (continued)

Pump Model	SKC 35304		SKC 35287	
	Pre (L/min)	Post (L/min)	Pre (L/min)	Post (L/min)
1	2.502	2.500	2.491	2.503
2	2.488	2.498	2.486	2.484
3	2.518	2.498	2.508	2.500
4	2.526	2.503	2.490	2.482
5	2.535	2.505	2.511	2.515
6	2.518	2.510	2.508	2.490
7	2.513	2.499	2.480	2.504
8	2.521	2.520	2.492	2.500
9	2.494	2.500	2.521	2.507
10	2.529	2.524	2.517	2.496
Average	2.514	2.506	2.500	2.498
SD	0.01523	0.00939	0.01420	0.01035
CV	0.606%	0.375%	0.568%	0.414%
Average Flow	2.510		2.499	

Air pumps where pre and post calibrated for each run with BIOS Defender 510-M.

Table XIX. Pre and Post Calibration of Pumps for Generation at RPM 1.6

Pump Model	SKC 35306		SKC 35287		MSA A3-45690	
	Pre (L/min)	Post (L/min)	Pre (L/min)	Post (L/min)	Pre (L/min)	Post (L/min)
1	2.507	2.512	2.490	2.489	2.488	2.476
2	2.521	2.495	2.502	2.485	2.489	2.466
3	2.485	2.505	2.490	2.477	2.492	2.465
4	2.501	2.506	2.493	2.470	2.488	2.463
5	2.527	2.502	2.511	2.460	2.498	2.465
6	2.523	2.250	2.506	2.498	2.501	2.463
7	2.522	2.505	2.486	2.491	2.490	2.462
8	2.524	2.485	2.504	2.457	2.496	2.464
9	2.518	2.509	2.505	2.467	2.488	2.463
10	2.493	2.496	2.483	2.474	2.488	2.464
Average	2.512	2.476	2.497	2.477	2.492	2.465
SD	0.01462	0.08002	0.00942	0.01367	0.00487	0.00401
CV	0.582%	3.231%	0.377%	0.552%	0.196%	0.163%
Average Flow	2.494		2.487		2.478	

Table XIX. Pre and Post Calibration of Pumps for Generation at RPM 1.6 (continued)

Pump Model	MSA A3-45691		MSA A3-45687	
	Pre (L/min)	Post (L/min)	Pre (L/min)	Post (L/min)
1	2.514	2.498	2.520	2.487
2	2.518	2.501	2.517	2.476
3	2.519	2.500	2.506	2.485
4	2.518	2.500	2.505	2.479
5	2.520	2.498	2.513	2.477
6	2.518	2.499	2.502	2.479
7	2.510	2.514	2.513	2.483
8	2.515	2.512	2.502	2.473
9	2.524	2.496	2.513	2.485
10	2.513	2.509	2.514	2.476
Average	2.517	2.503	2.510	2.480
SD	0.00386	0.00640	0.00645	0.00462
CV	0.153%	0.256%	0.257%	0.186%
Average Flow	2.510		2.495	

Appendix G: Critical Orifice Calibration

Critical orifices calibrated with BIOS Defender 510-M.

Table XX. Calibration of Critical Orifices.

	TI	T2	T3	T4	T5	T6	T7	T8
	3.351	3.398	3.349	2.202	2.239	2.178	2.253	2.277
	3.349	3.396	3.349	2.203	2.238	2.176	2.251	2.277
	3.348	3.396	3.349	2.203	2.235	2.179	2.253	2.279
	3.349	3.396	3.349	2.205	2.240	2.178	2.253	2.279
	3.347	3.396	3.349	2.206	2.239	2.180	2.255	2.279
	3.350	3.408	3.349	2.206	2.237	2.180	2.254	2.279
	3.348	3.396	3.349	2.206	2.236	2.176	2.257	2.270
	3.351	3.396	3.347	2.231	2.238	2.177	2.257	2.281
	3.348	3.396	3.351	2.229	2.238	2.177	2.257	2.283
	3.347	3.398	3.357	2.230	2.238	2.178	2.256	2.282
Average	3.349	3.398	3.350	2.212	2.238	2.178	2.255	2.279
SD	0.001	0.0037	0.0027	0.012	0.0015	0.0013	0.0022	0.0036
CV	0.04%	0.11%	0.08%	0.56%	0.07%	0.06%	0.10%	0.16%

Table XX. Calibration of Critical Orifices (continued)

	T9	IS 1	IS 2	IS 3
	2.273	3.980	3.995	3.976
	2.270	3.985	4.000	3.980
	2.271	3.984	4.000	3.978
	2.275	3.983	3.999	3.978
	2.273	3.984	4.001	3.977
	2.273	3.987	4.001	3.978
	2.274	3.984	4.000	3.977
	2.274	3.985	4.000	3.978
	2.274	3.985	4.000	3.980
	2.273	3.987	3.999	3.980
Average	2.273	3.984	3.999	3.978
SD	0.00143	0.00193	0.00186	0.00129
CV	0.06%	0.05%	0.05%	0.03%

Appendix H: Procedure for Generation of Gases in Exposure Chamber

This procedure was developed for the generation of gases using carbon dioxide.

1. Turn on the inhalation system and wait 5 minutes for its stabilization.
2. Obtain measurements of OM-1A and OM-1B. Calculate the air flowrate for each orifice meter using Equations 15 and 16 respectively. Use the average flowrate of both orifice meters as the flowrate inside the exposure chamber.
3. Connect the gas cylinder to the system. The injection point is located at the "T" junction where the fresh air take and duct from the vertical elutriator meet. Gas flow measurements can be obtained with a dry gas meter or a calibrated rotameter. Once the air flowrate and test gas flowrate are determined, the concentration at equilibrium inside the chamber can be predicted using Equation 4. Concentration at different points in time can be modeled using Equations 2 and 3. If the test material used is present in the atmosphere, background concentrations should be taken in consideration when developing the concentration model.
4. It is highly recommended to use a direct reading instrument to measure the gas concentration inside the chamber.
5. Performing "trial" gas generations prior an inhalation challenge study is strongly recommended. This will allow the researcher to be familiarized with the behavior of the test material and the exposure chamber during the generation of test atmospheres.

Appendix I: Procedure for Generation of Particles in Exposure Chamber

This procedure was developed for the generation of particulates. As stated before, the fly ash needs to be dried prior using it to avoid the formation of agglomerates.

1. Place the fly ash in tray in a way that the amount of fly ash barely covers the bottom of the tray. Dry the fly ash overnight in an oven at 200° C to reduce the moisture content in the fly ash. Let it cool at room temperature.
2. Once the fly ash had been dried, press the fly ash inside the dust cylinder of the Wright Dust Feeder using a 2-ton arbor press. This will reduce the variability of pressure when compacting the fly ash in the dust cylinder. For more information, please refer to the Wright Dust Feeder instruction manual.
3. Place the dust cylinder in the Wright Dust Feeder. Using a caliper, measure the distance of the fly ash plug in the dust chamber and make sure that once the dust chamber is closed, the scraper of the dust generator is close to the fly ash plug. Make sure that when screwing the dust chamber back into the dust generator, the scrapper does not touch the fly ash plug. If the scraper touches the fly ash plug during the step, it will affect the integrity of the compacted fly ash provoking the compacted fly ash to fall.
4. Turn on the blower of the exposure chamber. Turn on the TEOM and make sure that the door is closed. This instrument has a 30 minute warm up period. For more information about the operation of the TEOM, please refer to TEOM service manual.
5. Make sure the bypass of the dust generation is turned on (test material is

directed into a HEPA filter instead the exposure chamber). Turn on the dust generator and slowly open the valve of the nitrogen at the same time. The characterization of the chamber was made with the flowrate of nitrogen at 8.4 L/min (setting 30 at the rotameter). The flowrate of nitrogen will directly affect the particle size entering the chamber and the dust concentration inside the exposure chamber. Leave it running for 15 minutes to make sure the scraper of the dust generator is engaged in the fly ash plug and the generated initial cloud pulse is captured by the HEPA filter. Make sure the TEOM is in Operation Mode "OK 4".

6. Turn off the bypass into the exposure chamber. That is the moment when the generation of test material starts. Turn on the bypass to end the generation of test material.
7. For the measurements of particle size distributions while conducting generation of particles, please refer to the instruction manual of the QCM cascade impactor.

Appendix J: Concentration across Exposure Chamber

For determination of distribution of concentration across the exposure chamber, five consecutive runs were made. Dust concentrations were determined by gravimetric analysis using 37 mm open face cassettes with PVC filters. No target dust concentration was intended during this exercise.

Table XX. Concentrations across the Exposure Chamber

Filter	Run 1 ($\mu g/m^3$)	Run 2 ($\mu g/m^3$)	Run 3 ($\mu g/m^3$)	Run 4 ($\mu g/m^3$)	Run 5 ($\mu g/m^3$)
1	336	407	354	252	276
2	358	419	366	284	276
3	273	408	334	273	287
4	321	447	351	279	281
5	320	391	359	277	301
6	277	377	346	277	218
7	287	357	336	246	290
8	310	388	358	250	283
9	293	432	361	273	306
10	317	335	314	306	266
11	306	385	395	265	298
12	297	345	315	266	330

Appendix K: Calibration of Critical Orifices for Evenness of Concentration

Table XXI. Calibration of Critical Orifices for Evenness of Concentration

Critical Orifice	T1	T2	T3	T4	T5	T6	T7
	3.181	3.175	3.176	3.115	3.13	3.255	3.241
	3.178	3.164	3.17	3.113	3.13	3.254	3.253
	3.175	3.16	3.167	3.106	3.142	3.251	3.245
	3.170	3.163	3.168	3.112	3.124	3.252	3.254
	3.170	3.161	3.167	3.109	3.121	3.249	3.249
Average	3.175	3.1646	3.1696	3.111	3.1294	3.2522	3.2484
SD	0.00487	0.00602	0.00378	0.00354	0.00805	0.00239	0.00546
CV	0.15%	0.19%	0.12%	0.11%	0.26%	0.07%	0.17%

Table XXI. Calibration of Critical Orifices for Evenness of Concentration (continued)

T8	T9	T10	T11	T12
3.334	3.299	3.16	3.274	3.256
3.327	3.295	3.151	3.261	3.249
3.32	3.288	3.143	3.274	3.256
3.343	3.312	3.166	3.267	3.255
3.339	3.306	3.177	3.273	3.278
3.3326	3.3	3.1594	3.2698	3.2588
0.00924	0.00935	0.01316	0.00572	0.01112
0.28%	0.28%	0.42%	0.17%	0.34%

About the Author

Luis F. Pieretti received a Bachelor's Degree in Biology from Inter American University of Puerto Rico in 2001 and a M.S. in Industrial Hygiene from University of Puerto Rico in 2003. He started working as an industrial hygiene specialist for Johnson and Johnson in San Germán, PR until he entered the doctoral program at USF in 2005.

While in the Ph.D. program at the University of South Florida, Mr. Pieretti assisted the Environmental and Occupational Health graduate course and worked as a consultant for the USF SafetyFlorida OSHA Consultation Program.